agronomy

MDPI

Article

Remote Sensing-Assisted Estimation of Water Use in Apple Orchards with Permanent Living Mulch

Susana Ferreira [1,*], Juan Manuel Sánchez [1], José Manuel Gonçalves [2], Rui Eugénio [3] and Henrique Damásio [3]

[1] Instituto de Desarrollo Regional, UCLM Universidad de Castilla-La Mancha, 02071 Albacete, Spain; juanmanuel.sanchez@uclm.es
[2] IPC Instituto Politécnico de Coimbra, Escola Superior Agrária de Coimbra, CERNAS—Research Center for Natural Resources, Environment and Society, 3045-601 Coimbra, Portugal; jmmg@esac.pt
[3] ARBVL Associação de Regantes e Beneficiários do Vale do Lis, Quinta do Picoto, 2425-492 Leiria, Portugal; eugenio-rui@sapo.pt (R.E.); hdamasio71@gmail.com (H.D.)
* Correspondence: susana.carvalho@alu.uclm.es

Abstract: Orchards are complex agricultural systems with various characteristics that influence crop evapotranspiration (ET_c), such as variety, tree height, planting density, irrigation methods, and inter-row management. The preservation of biodiversity and improvement of soil fertility have become important goals in modern orchard management. Consequently, the traditional approach to weed control between rows, which relies on herbicides and soil mobilization, has gradually been replaced by the use of permanent living mulch (LM). This study explored the potential of a remote sensing (RS)-assisted method to monitor water use and water productivity in apple orchards with permanent mulch. The experimental data were obtained in the Lis Valley Irrigation District, on the Central Coast of Portugal, where the "Maçã de Alcobaça" (Alcobaça apple) is produced. The methodology was applied over three growing seasons (2019–2021), combining ground observations with RS tools, including drone flights and satellite images. The estimation of ET_a followed a modified version of the Food and Agriculture Organization of the United Nations (FAO) single crop coefficient approach, in which the crop coefficient (K_c) was derived from the normalized difference vegetation index (NDVI) calculated from satellite images and incorporated into a daily soil water balance. The average seasonal ET_a (FAO-56) was 824 ± 14 mm, and the water productivity (WP) was 3.99 ± 0.7 kg m^{-3}. Good correlations were found between the K_c's proposed by FAO and the NDVI evolution in the experimental plot, with an R^2 of 0.75 for the entire growing season. The results from the derived RS-assisted method were compared to the ET_a values obtained from the Mapping Evapotranspiration at High Resolution with Internalized Calibration (METRIC) surface energy balance model, showing a root mean square (RMSE) of ±0.3 mm day^{-1} and a low bias of 0.6 mm day^{-1}. This study provided insights into mulch management, including cutting intensity, and its role in maintaining the health of the main crop. RS data can be used in this management to adjust cutting schedules, determine K_c, and monitor canopy management practices such as pruning, health monitoring, and irrigation warnings.

Keywords: apple orchard; crop water management; Maçã de Alcobaça (Alcobaça apple); permanent living mulch; remote sensing

check for updates

Academic Editor: Baohua Zhang

Received: 11 December 2024
Revised: 22 January 2025
Accepted: 25 January 2025
Published: 28 January 2025

Citation: Ferreira, S.; Sánchez, J.M.; Gonçalves, J.M.; Eugénio, R.; Damásio, H. Remote Sensing-Assisted Estimation of Water Use in Apple Orchards with Permanent Living Mulch. *Agronomy* **2025**, *15*, 338. https://doi.org/10.3390/agronomy15020338

Copyright: © 2025 by the authors. Licensee MDPI, Basel, Switzerland. This article is an open access article distributed under the terms and conditions of the Creative Commons Attribution (CC BY) license (https://creativecommons.org/licenses/by/4.0/).

1. Introduction

Apple orchards are a major perennial crop worldwide. Over the last decade, global apple production has increased by nearly 9 million tons, from 38 to 47 million tons, while

the harvested area has remained stable at approximately 2 million hectares [1]. In Portugal, the latest statistics from 2023 indicate a cultivated area of 14 thousand hectares, yielding 292 thousand tons, ranking apples as the country's fifth most produced commodity [2]. One prominent apple-producing region is the Central West Coast, known for the Alcobaça apple (Maçã de Alcobaça), a collective brand representing a group of fruits qualified under the Protected Geographical Indication (PGI) since 1996. This brand includes nine apple varieties: Casa Nova, Golden Delicious, Red Delicious, Gala, Fuji, Granny Smith, Jonagold, Reineta, and Pink. These apples are distinguished by high consistency, crunchiness, elevated sugar content, and unique bittersweet taste and aroma [3].

During the growing season, rainfall is insufficient to meet the evapotranspiration demands of apple trees, resulting in significant water scarcity, especially during critical fruit growth stages. This water shortage directly affects both yield and quality, making irrigation essential for maintaining optimal growth conditions. In contrast to traditional cultivation methods in marginally irrigated areas, effective irrigation management is crucial for modern orchards. A sound understanding of soil water balance and crop evapotranspiration allows for efficient water and nutrient distribution, helping to mitigate the effects of moisture stress. This not only enhances production quality but also improves fruit size and sensory, nutritional, and preservation characteristics. Addressing moisture scarcity through precise irrigation strategies is key to ensuring sustainable orchard productivity and maintaining fruit quality under varying climatic conditions. Permanent living mulch (LM) is a widely adopted orchard management practice [4,5]. According to some authors' definition, LM consists of cover crops planted before or alongside a main crop and maintained as a living ground cover throughout the growing season [6]. In practice, this involves establishing perennial forage legumes and grasses to maintain soil protection as a (semi-)permanent ground cover. LM is a comprehensive system, integrating concepts of intercropping, cover cropping, undersowing, and mulching, into orchard management [7]. Compared to conventional tillage, LM offers several advantages due to continuous soil coverage, significantly enhancing soil quality and orchard sustainability. LM helps prevent soil erosion and compaction while enriching soil fertility. Vegetation under tree canopies, for instance, can accumulate nitrogen in green parts, some of which returns to the soil after mowing [8]. Additional benefits include improved soil structure, reduced salinity, decreased nutrient leaching, and enhanced water retention capacity [9–11]. LM also regulates the orchard microclimate by lowering soil temperatures, insulating the soil, and mitigating extreme temperature fluctuations. This contributes to reducing plant stress [12], slowing wind speed at the soil surface, and retaining soil moisture [13], all of which are critical for sustainable orchard management.

Beyond soil health and microclimate regulation, LM contributes to pest and weed control, production improvement, and microbial community diversity, supporting beneficial predators in orchards and reducing the need for chemical interventions. Intercropping with flowering plants enhances floral diversity, which is essential for pollinators such as bees, thus contributing to ecosystem services [14,15]. Weeds threaten crops by competing for essential resources, such as light, water, and nutrients, and through allelopathic effects, they can increase the risk of diseases and pests, including rodents and frost damage during flowering [16,17]. Effective weed management is vital for maintaining healthy fruit trees and includes methods such as herbicide application, tillage, mowing, flame weeding, mulching, and the use of cover crops, including LM, which have been recognized for their ability to limit weed populations in orchards [18,19]. The European Union, acknowledging the environmental benefits of weeds, promotes eco-schemes in its 2023–2027 Common Agricultural Policy (CAP), supporting farmers in adopting practices that minimize agriculture's negative impacts on the environment and climate [20].

Furthermore, LM positively impacts fruit quality and productivity, which are key objectives in orchard management [21]. Recent studies show that permanent LM in apple orchards enhances tree productivity and fruit quality [22]. Other studies confirm that grass mulching positively impacts fruit quality indicators, such as soluble sugar content [23]. A comprehensive meta-analysis confirmed that grass cultivation in orchards positively impacts overall fruit quality [24]. In pear orchards, green cover crops have been found to increase fruit nutritional value [25], while other studies noted that grass cultivation can reduce fruit acidity in orchards [26,27]. Additionally, LM increases microbial diversity by introducing organic matter, serving as a food source for bacteria and fungi, thereby enhancing microbial biomass [28,29]. For instance, leguminous plants in LM systems foster nitrogen-fixing bacteria, like *Rhizobium*, which enhances soil nitrogen and supports the proliferation of beneficial microbes [30]. These microbes improve nutrient absorption, especially phosphorus, and protect against soil-borne pathogens [31].

Following the Food and Agricultural Organization of the United Nations (FAO) methodology, crop water requirements can be estimated by multiplying reference evapotranspiration (ET_o) with the crop coefficient (K_c) to estimate actual evapotranspiration (ET_a) [32]. Calculating ET_a is critical for irrigation schemes, and it enhances water management in the field and provides insight into the hydrological cycle, a pressing need in the context of global climate change [33]. Experimental methods, like lysimeters [34] and eddy covariance [35], have been used in orchards to determine K_c values through direct ET measurement, though these methods are generally limited to small areas and are challenging to extrapolate due to the variability in land surfaces [36] and the differences in crops, soil types, and weather conditions [37]. To overcome these limitations, remote sensing (RS) models and algorithms have been developed to quantify ET_a in apple orchards, complementing ground-based data with more comprehensive spatial insights [38,39].

K_c values reflect factors such as crop growth characteristics, soil properties, and management practices [40]. Both single and dual crop coefficient approaches have been widely adopted. The single crop coefficient combines the effects of crop transpiration and soil evaporation into a single value [41]. In contrast, the dual crop coefficient separates K_c into two components: the basal crop coefficient (K_{cb}), which represents crop transpiration under standard conditions, and the soil evaporation coefficient (K_e), which accounts for water evaporation from the soil surface. This separation allows for a more detailed estimation of evapotranspiration. In our study, we used the single crop coefficient approach, as mature trees provided substantial soil coverage during the growing season, significantly reducing direct soil evaporation.

RS methods, especially those using vegetation indices (VIs), such as the normalized difference vegetation index (NDVI), have become viable alternatives for estimating K_c values. The NDVI, despite its limitations (e.g., saturation effects and soil reflectance interference [42]), was chosen for this study due to its consistent use in the existing literature [43,44]. The NDVI utilizes two spectral bands: chlorophyll absorption in the red band (0.62–0.69 μm) and high reflectance from plant materials in the near-infrared (NIR) band (0.75–1.3 μm) [45] and is calculated by taking the normalized difference between these two bands, expressed mathematically as (NIR–RED)/(NIR + RED) [46,47]. The NDVI ranges from −1 to 1; high levels of photosynthetic activity correlate with lower reflectance values in the red band and higher values in the NIR band. This distinction allows for effective differentiation between vegetation and other land surfaces. Generally, bare soil displays NDVI values of 0.1 to 0.2, while vegetated areas show values from 0.2 to 1, reflecting the different light reflectance properties of plants [48]. The NDVI serves as an indicator of the photosynthetic activity in plant canopies, offering valuable insights into the dynamics of vegetation over the growing season [49] and aiding in the estimation of crop yield in conjunction with other parameters [50].

The adoption of $K_c(_b)$-VI methods to calculate crop coefficients is based on the similarities of K_c (and K_{cb}) and the VIs. In recent decades, these methods have gained widespread acceptance for estimating crop coefficients on various crops, including rice [51,52], maize [53], sorghum [54], and grapes [55]. The overall conclusion from these investigations highlighted the significant utility of reflectance-based models for crop irrigation management. Operational tools, such as the HidroMORE© platform developed by the University of Castilla-La Mancha in Spain, have been developed to integrate time series of satellite data into the application of FAO-56 methodology for determining water availability for crops [56]. This operational tool has been utilized in numerous studies [57,58], including water management assessments at the scale of Water Users' Associations (WUAs) [59–61].

This study established a method for estimating ET_a in apple orchards using a temporal series of NDVI satellite images provided by SPIDERwebGIS© from the University of Castilla-La Mancha, Spain, thus creating a process that can be broadly applied to enhance irrigation and crop management practices. This approach was evaluated by comparing the results with those obtained from the Mapping Evapotranspiration at High Resolution with Internalized Calibration (METRIC) model for the study site in the Lis Valley Irrigation District (LVID). Additionally, we studied the effects of permanent mulching on soil moisture. The significance of this research lies in its potential to improve water use efficiency and crop productivity in apple orchards, offering a more sustainable approach to irrigation management.

2. Materials and Methods

2.1. Site Description

This study was conducted in a drip-irrigated apple orchard (*Malus domestica* Mill., cultivars Fuji and Gala) located within the LVID, Leiria, on Portugal's Central Coast (39°51′12.47″ N, 8°52′8.45″ W) (Figure 1). This study spanned the 2019, 2020, and 2021 growing seasons. The region's climate is classified as Mediterranean semi-arid (Csb) according to the Köppen–Geiger climate system [62], characterized by mild winters and temperate summers. The average annual precipitation is 790 mm, primarily concentrated from October to March (Figure 2). The region's mean annual temperature is 14.9 °C, with an average maximum of 20.6 °C and a minimum of 10 °C [63].

The study area's soils are alluvial origin, with variable textures, including clayey, sandy–clay, and sandy soils [64]. While these soils have high agricultural value, some exhibit drainage issues.

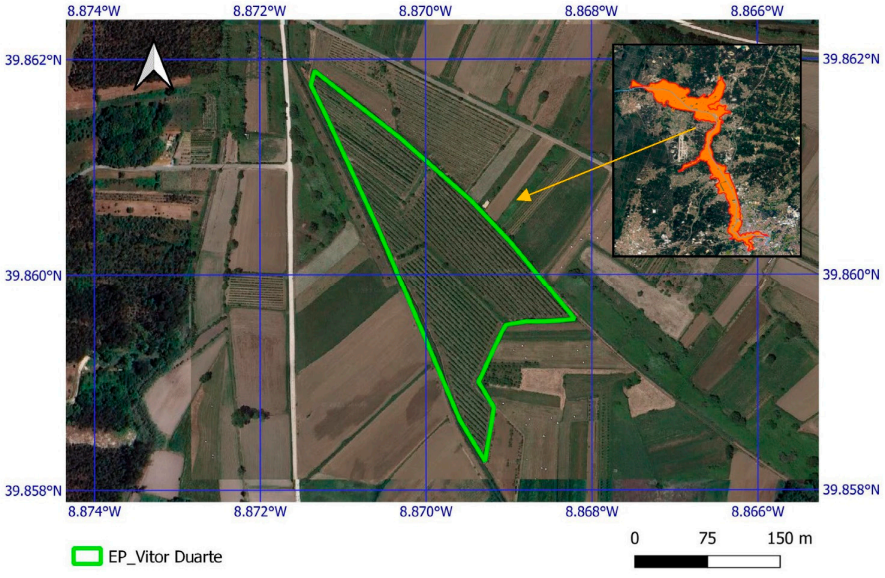


Figure 1. Geographic location of the LVID. The red line marks the LVID boundary, the blue line traces the course of the Lis River, and the orange lines outline the plot boundaries. The green area in the lower

left corner represents the layout of the "Vitor Duarte Experimental Plot" (source: Google Earth, https://earth.google.com, accessed on 12 September 2024).

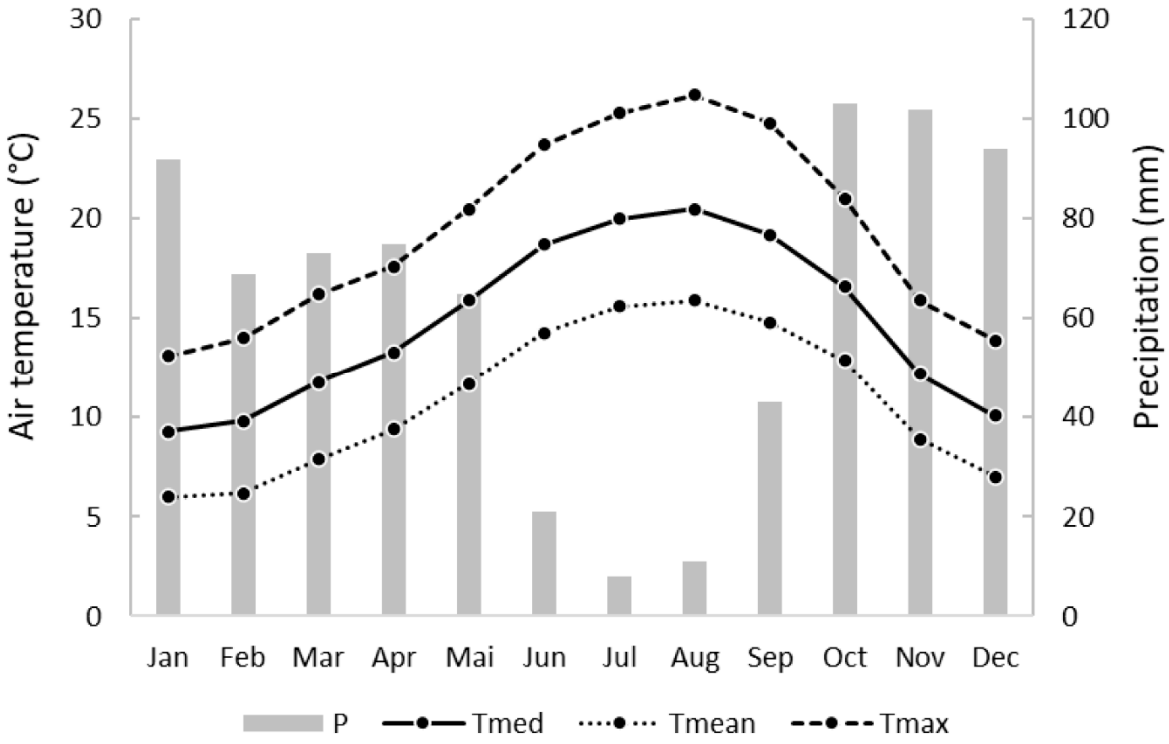


Figure 2. Average monthly air temperature and precipitation on the LVID (P—precipitation; T_{min}—minimum air temperature; T_{mean}—mean air temperature; T_{max}—maximum air temperature) (adapted from [65]).

Fruit production, including apples, pears, and small fruits, occupies nearly 20 hectares of the total irrigated area in the LVID [66], with further expansion anticipated in the near future. Apple orchards in this area are primarily managed by a single-family enterprise. The experimental plot, known as the "Vitor Duarte Experimental Plot", spans 3 hectares. Located in Leiria within the Alcobaça Apple region, this plot falls under the PGI designation. Apple trees were planted in 2014, in a high-density arrangement of 1 m × 4 m, yielding an average of 30 tons per hectare annually. The trees are grown to a typical height of 3 to 4 m, allowing for efficient harvesting and management.

The soil at the plot has a silty clay texture, containing 2.6% organic matter and a pH of 8.1. Soil electrical conductivity (EC) measures at 0.21 dS m^{-1}, indicating no salinity issues. Drip irrigation is provided across seven sectors, beginning in mid-May or June and concluding a week before harvest. Drip irrigation is managed empirically, based on observed crop needs, soil conditions, climatic forecasts, and the grower's observations. The irrigation plan is adapted accordingly. Unfortunately, digital water meters were not available, and only accumulated total irrigation was known, by estimation. Drainage is managed with a network of ditches to maintain a water table at a level that supports root zone aeration while ensuring sufficient soil moisture availability for crop growth. Fertilization, focusing on phosphorus and potassium, is adjusted annually through soil analyses to ensure the appropriate application of nutrients. Fertilization is applied via fertigation, with orchard management targeting high yield, fruit size, and quality.

The availability of irrigation and yield data enables the calculation of water productivity (WP) and water use efficiency (WUE). WP is defined as crop yield per m^3 of water applied, considering effective precipitation and irrigation for irrigated areas. WP (kg m^{-3}) is calculated by dividing yield (kg ha^{-1}) by total water applied (precipitation plus

irrigation, inm^3 ha^{-1}). WUE is calculated as the ratio of total actual evapotranspiration (ET_a, inm^3 ha^{-1}) to the total volume of water applied.

The soil is naturally occupied by spontaneous Poaceae and Fabaceae species (Figure 3), which are mowed three times a year (1) in January–February, when pruning residues are incorporated into the soil, (2) in May, mid-spring, and (3) in August, prior to harvest. The primary weed issue is *Convolvulus arvensis*, which climbs the apple trees, wrapping around trunks and potentially impacting yields. Main phytosanitary issues arise from *Venturia inaequalis* (apple scab) and powdery mildew, and they are managed with treatments using a towable atomizer. The farmer also controls *Drosophila melanogaster* populations through mass trapping with food baits containing attractants and insecticide along the orchard borders. In recent years, an increase in nesting birds—pheasants and blackbirds—and beneficial insects, such as *Chrysoperla carnea*, has been observed. This is a direct consequence of the implementation of LM, which enhances biodiversity by providing shelter, nesting habitats, and food resources while also contributing to improved ecological balance within the orchard ecosystem.



Figure 3. Permanent mulching in the orchard, represented by the herbs growing between the rows of apple trees (photo taken on 12 June 2024).

2.2. Soil Moisture and Groundwater

Soil moisture and groundwater measurements were conducted at three strategic locations along the planting line (at the beginning, middle, and end) using a portable TDR probe, model H2D IMKO (Figure 4b). This probe allowed for simultaneous measurements of EC and soil moisture content, with readings taken during the growing seasons from June to August in both 2019 and 2020 at depths of 20, 30, and 50 cm. EC is an important parameter for assessing soil salinity, as high EC values can indicate elevated levels of soluble salts, which may affect water availability to the apple trees. Monitoring EC helps detect potential salinity stress that could impact plant health and productivity.

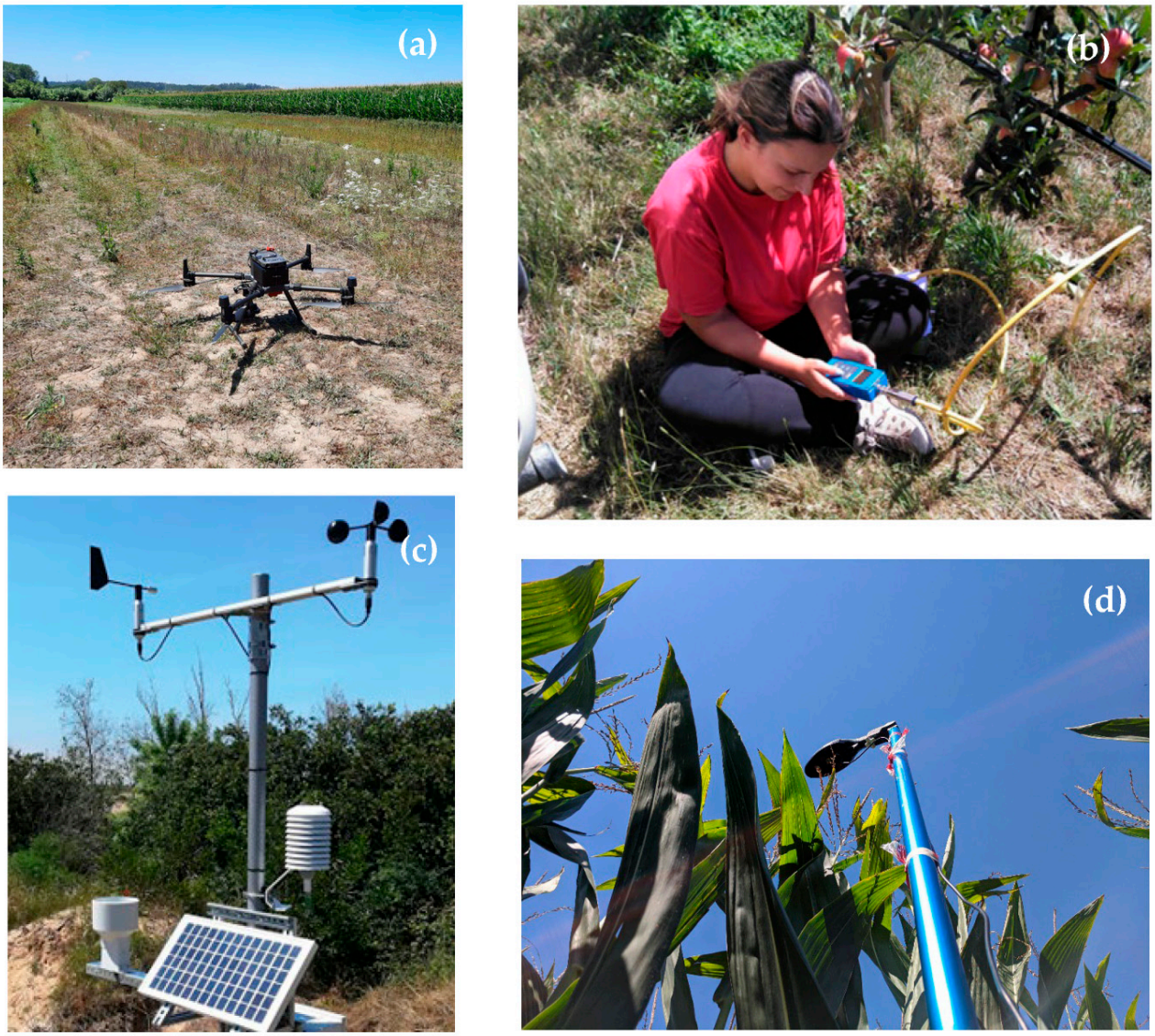


Figure 4. Drone used for the data collection flight (**a**), measurement of soil moisture with a portable probe (**b**), automatic agrometeorological station (**c**), and a GreenSeeker Handheld Crop Sensor being used in a maize field (**d**), illustrating the methodology employed for NDVI measurements in this study. Although the image was taken in a maize field, the same approach was applied to the apple orchards.

The available water capacity (AWC) was calculated by determining the volumetric field capacity, which was measured at 32%, and subtracting the wilting coefficients: 18, 19, and 20% for depths of 20, 30, and 50 cm, respectively. This calculation provided a clear understanding of the soil's moisture retention potential at each depth. Soil water storage (AWS) was computed by integrating the moisture content data collected from the TDR probe over time, reflecting the actual water storage in the soil during different periods of the growing seasons. Comparing AWS with AWC enabled the identification of periods with sufficient water availability and potential drought stress, thus informing irrigation practices.

To monitor groundwater depth, a piezometer was installed at a depth of 3 m, strategically located near the observation line to assess fluctuations in the water table. Piezometer readings were recorded periodically, providing valuable insights into groundwater level variations throughout the seasons.

2.3. Weather Station, Reference, and Actual Evapotranspiration Through the FAO-56 Methodology

The weather conditions during the three study seasons were monitored using an automated agrometeorological station (N 39°51′22.32″, W 8°50′56.44″) located 2.5 km from the experimental plot (Figure 4c). Sensors were installed at a height of 2 m above ground level, and meteorological data were recorded hourly, following methodologies established in prior studies [67].

The initial method for estimating the orchard's ET_a was based on FAO-56 ($ET_a = K_c \times ET_o$) [68]. Daily ET_o values were calculated using the FAO-56 Penmann–Monteith reference ET equation for grass [32] as follows:

$$ET_o = \frac{0.408\,\Delta(R_n - G) + \gamma\frac{900}{T+273}u_2\,(e_s - e_a)}{\Delta + \gamma(1 + 0.34u_2)} \quad (1)$$

where ET_o is the reference evapotranspiration (mm day^{-1}), R_n is the net radiation (MJ m^{-2} d^{-1}), G is the soil heat flux density (MJ m^{-2} d^{-1}), T is the air temperature at a 2 m height (°C), u_2 is the wind speed at a 2 m level (m s^{-1}), e_s is the saturation vapor pressure of the air (kPa), e_a is the actual vapor pressure (kPa), Δ is the slope of the vapor pressure curve (kPa $°C^{-1}$), and γ is the psychrometric constant (kPa $°C^{-1}$).

The lengths of the apple tree growing phases (initial, development, middle, and late) were identified in Table 11 of the FAO-56 manual, with a growth cycle of 230 days. Crop coefficients for each growth stage (Kc_{ini}, Kc_{mid}, and Kc_{end}) were derived from the FAO-56 guidelines for fruit trees (Table 12, [32]) using values for apple trees planted in active ground cover with no frosts, in accordance with the conditions at the experimental site.

2.4. Actual Evapotranspiration from METRIC

For this study, a total of 27 clear-sky Landsat 8 images were analyzed, spanning the apple growing season and encompassing the four growth stages (I—initial, II—development, III—middle, and IV—late), as defined in Table 11 of FAO-56 [32]. The dataset included 8 images from 2019, 9 from 2020, and 10 from 2021 (Table 1). The images were processed using the EEFlux platform (version 0.20.17), accessible at https://eeflux-level1.appspot.com, as of September 2024. EEFlux serves as a fully automated framework for the METRIC algorithm, implemented on the Google Earth Engine, designed to estimate RS-based ET [69]. The platform utilizes thermal and shortwave bands from Landsat to calculate ET_a, using parameters such as albedo, the vegetation index, and land surface temperature [70]. The METRIC-EEFlux images were calibrated using alfalfa reference ET, with gridded weather data employed to compute the fraction of reference ET (ET_oF). This fraction is applied to extrapolate instantaneous ET (ET_{ins}) for each pixel during the satellite overpass. Instantaneous ET is derived from the latent heat flux using the following equation:

$$ET_{ins} = 3600 \times LE/(\lambda \times \rho) \quad (2)$$

where ET_{ins} is the instantaneous ET (in mm h^{-1}), LE is the latent heat flux (W m^{-2}), "λ" is the latent heat of vaporization (in J kg^{-1}), and ρ is the density of water (kg m^{-3}).

The fraction of reference ET (ET_oF) is calculated by the following:

$$ET_oF = ET_{ins}/ET_{oins} \quad (3)$$

where ET_{oins} is the instantaneous reference evapotranspiration under standard climatic conditions.

Table 1. Acquisition dates of Landsat 8 images used in this study along with their corresponding crop growth stage.

2019		2020		2021	
IAD	**AGS**	**IAD**	**AGS**	**IAD**	**AGS**
18 Apr.	II	19 Mar.	I	22 Mar.	I
04 May	II	6 May	II	7 Apr.	II
21 Jun.	III	22 May	II	23 Apr.	II
24 Aug.	III	7 Jun.	II	25 May	II
9 Sep.	III	9 Jul.	III	10 Jun.	II
25 Sep.	IV	26 Aug.	III	26 Jun.	III
11 Oct.	IV	11 Sep.	III	12 Jul.	III
27 Oct.	IV	13 Oct.	IV	28 Jul.	III
		29 Oct.	IV	13 Aug.	III
				29 Aug.	III

IAD—image acquisition date; AGS—apple growth stage.

The daily ET_a for each pixel is then calculated as follows:

$$ET_a = ET_oF \times ET_o \quad (4)$$

Due to the 30 m level of detail in Landsat 8, multiple pixels within the study plot were covered. For analysis, mean values were extracted from a 3 × 3-pixel grid using QGis software (version 3.36.1 Zurich) for image processing.

2.5. Satellite and UAV Acquisition, Processing, and Ground Measurements for the NDVI

Satellite images from the Landsat 8 and Sentinel-2A and -2B constellations (USGS and EU Copernicus Program, respectively) were used to derive the NDVI. Sentinel-2 provides Visible and Near-Infrared (VNIR) data at spatial resolutions of 10–20 m, with a revisit interval of five days at the equator. Landsat 8, with a temporal resolution of 16 days, includes the Operational Land Imager (OLI) sensor, which captures images at a 30 m resolution in visible, NIR, and SWIR bands, along with the Thermal Infrared Sensor (TIRS) at a 100 m resolution. The launch of Landsat 9 in September 2021 further reduced revisit intervals, enhancing the program's temporal coverage. The path/row designation for Landsat images is 204/32, while for Sentinel-2, it is "TILE29TNE".

Satellite datasets were managed using the SPIDERwebGIS© platform (http://maps.spiderwebgis.org/webgis/, accessed on 30 September 2024), referred to here as SPIDER. This platform was developed by the University of Castilla-La Mancha, Spain. Orthorectified Surface Reflectance imagery (Bottom Of Atmosphere: BOA) was used to ensure consistent surface reflectance across different acquisition dates. The platform enables users to visually assess temporal changes in surface reflectance, vegetation indices, and water requirements. In this study, the orchard was identified within the SPIDER platform, and five sample points within the plot were selected for the period from 2019 to 2021. The NDVI was calculated as the average of these five points for each acquisition period, ensuring more reliable results. For dates without satellite images, NDVI values were linearly interpolated between adjacent time points to provide continuous daily temporal NDVI data.

Additionally, UAV data were collected on 26 July 2021, during favorable weather conditions (clear skies and calm winds) using the DJI Matrice 350 drone (Figure 4a). The drone was equipped with a Zenmuse X5 camera for RGB imaging (DJI, Shenzhen, China) and a MicaSense REDEdge-M Multispectral sensor (MicaSense, Seattle, WA, USA). The sensor captures imagery in key spectral bands: blue (475 nm), green (560 nm), red (668 nm), red edge (717 nm), and NIR (842 nm), with a ground sample distance of 7.21 cm per pixel.

Radiometric corrections were performed based on the camera, sun irradiance, and sun angle using DLS IMU. The drone followed a predefined grid flight plan with 25 m separation between flight lines, 75% overlap, and 70% sidelap, maintaining an altitude of 100 m and a speed of 7.5 m s^{-1}. A calibration target was used for quick calibration before the flight. Data from the UAV flight images, including orthorectification, atmospheric correction, and the creation of vegetation index maps, were processed using Pix4D software, version 4.8.2 Pix4D S.A., Prilly, Switzerland). The NDVI values were derived from drone imagery processed in QGIS (version 3.36.1). Regions of interest (ROIs) were manually delineated based on visual inspection of the raster dataset, distinguishing apple trees from inter-row grass cover. The "Zonal Statistics" tool was used to extract the mean and standard deviation of NDVI values for each ROI, ensuring precise differentiation between the two classes.

To validate the satellite-derived NDVI, GreenSeeker Handheld Crop Sensor measurements were taken at three points within the plot during the 2020 campaign (Figure 4d). Given the significant height of the trees, an extender was required to cover the full canopy and ensure accurate measurements. The sensor was held over the canopy at an average height of 1 m above the crop, and a remote switch enabled precise NDVI capture. The average NDVI was calculated by applying a weighting factor of 0.25 for the trees and 0.75 for the mulch, based on the spatial arrangement within the plot. Given that the row spacing is 4 m, with the trees occupying approximately 1 m and the mulched area covering the remaining 3 m, this weighting approach reflects the proportionate ground coverage of each component. This method allows for an accurate representation of the overall NDVI by accounting for the relative contributions of the tree canopy and ground cover vegetation.

2.6. Model Performance Evaluation: BIAS, RMSE, and Linear Regression Analysis

To evaluate the performance of the ET_a estimation models, statistical metrics such as BIAS (Mean Bias Error), RMSE (Root Mean Square Error), and linear regression were employed. These metrics were used to compare the actual ET_a values derived from ground-based measurements with those estimated using remote sensing techniques.

BIAS was used to assess the systematic errors in the model's predictions, with negative values indicating underestimation and positive values indicating overestimation of ETa. RMSE provided a measure of the overall accuracy of the model by quantifying the average magnitude of the errors, considering both the magnitude and the direction of errors.

In addition, linear regression was performed between the mean ET_a values provided by the METRIC model and the ET_a values calculated from the derived Kc = Kc (NDVI) relationship. This analysis helped to determine the degree of agreement between the observed and estimated ET_a values, further validating the model's accuracy.

These statistical analyses allowed for a comprehensive evaluation of the model's performance, offering valuable insights into the reliability and accuracy of the remote sensing-based ET_a estimation methods.

3. Results

3.1. Meteorological Data

Table 2 presents the monthly meteorological data for the apple growing seasons from 2019 to 2021 (mid-March to the end of October). Air temperatures ranged from 11.2 to 19.7 °C, with wind speeds varying between 1.4 and 2.6 m s^{-1}. Cumulative precipitation reached 340.4 mm in 2019, 334.2 mm in 2020, and 370.2 mm in 2021. Although the growing seasons were generally typical of average weather conditions on the Central Coast of Portugal, precipitation levels were lower than historical records for these years [71–73].

Table 2. Summary of monthly meteorological variables during the 2019, 2020, and 2021 apple growing seasons.

Season	T_{mean} (°C)			RH_{mean} (%)			u_2 (m s^{-1})		
Month	2019	2020	2021	2019	2020	2021	2019	2020	2021
Mid-March	14.2	11.2	12.0	65.0	84.4	75.1	2.6	1.8	1.8
April	13.8	13.8	14.5	86.4	87.3	87.0	2.5	1.8	1.6
May	17.3	17.4	14.8	78.1	84.2	83.3	2.4	1.8	2.0
June	16.5	17.6	17.1	78.4	83.0	85.3	2.1	2.1	2.1
July	19.2	19.7	18.6	83.1	82.6	84.1	2.2	2.0	2.2
August	19.4	19.5	18.6	83.4	86.4	87.1	2.1	2.1	1.9
September	17.9	18.4	18.9	81.2	84.3	86.2	1.6	1.6	1.6
October	15.5	14.4	16.1	86.5	87.8	88.2	1.7	1.6	1.4
Season	**R_s (MJ m^{-2} day^{-1})**			**P (mm)**			**ET_o (mm day^{-1})**		
Month	2019	2020	2021	2019	2020	2021	2019	2020	2021
Mid-March	19.2	13.8	17.8	1.0	24.0	0	3.3	2.0	2.8
April	19.4	15.8	16.7	158.0	96.0	111.4	2.9	2.5	2.6
May	26.9	22.1	22.9	20.4	45.8	46.8	4.4	3.8	3.5
June	23.8	23.7	23.0	20.6	10.2	28.2	4.0	3.9	3.7
July	20.5	26.0	23.2	10.8	0.2	8.0	3.8	4.6	4.0
August	20.9	21.4	22.4	17.0	18.4	4.0	3.8	3.7	3.7
September	16.8	16.9	16.6	29.4	49.8	55.6	3.1	3.1	2.9
October	11.0	12.0	12.3	83.2	89.8	116.2	1.8	1.8	2.0

T_{mean} is the mean air temperature, RH_{mean} is the mean relative humidity, u_2 is the wind speed measured at 2 m height, R_s is the global solar radiation, P is the monthly total precipitation, and ET_o is the reference evapotranspiration calculated with the FAO-56 PM equation.

In terms of temperature, heatwaves occurred in March 2019 and again in 2021, with May being notably hot and dry in both 2019 and 2020 (2020 marked as the hottest year since 1931). In contrast, 2021 saw unusually low minimum temperatures. The summer of 2019 was cool and dry, recording the lowest minimum air temperature in the past 40 years; June 2019 was the coldest since 2000 [71]. July and September 2020 also experienced heatwaves, while October of that year was exceptionally cold [72]. The summer of 2021 featured average temperatures but showed a precipitation deficit [73].

Relative humidity began increasing in April, with 2019 recording particularly low values, especially in mid-March. Global solar radiation was consistent across the three years, ranging from 12.3 to 26.9 MJ m^{-2} day^{-1}. Evapotranspiration demand was higher from May to August across all studied years, with an average of 4 mm day^{-1}.

3.2. Soil Water Dynamics

Figure 5 presents the groundwater levels recorded for the apple orchard during 2019 and 2020, which showed relatively high values, indicating adequate water availability for the crop. Note that no measurements were conducted in 2021. In 2019, a significant drop in groundwater levels was observed in August, with measurements reaching 0.15 m below the soil surface. However, this was followed by a recovery to 0.38 m in September, suggesting that the water supply was temporarily low but not critically so, remaining adequate for supporting plant growth. In 2020, groundwater levels ranged from 0.50 m in June to a peak of 0.89 m in August. These values remained within an acceptable range, with no signs of prolonged water stress affecting the apple trees. The absence of significant fluctuations in 2020 suggests effective water management and favorable climatic conditions. The recharge effect of groundwater was strong during the study period, particularly in 2020 when the

groundwater table remained relatively stable, contributing to the overall water availability for the crop. The presence of shallow groundwater likely reduced the irrigation needs, as the water table provided additional moisture to the root zone, enhancing the orchard's water supply. Additionally, the groundwater salinity level was 0.83 dS m^{-1}. Overall, the data indicate that the groundwater levels were sufficient to support apple growth without causing stress.

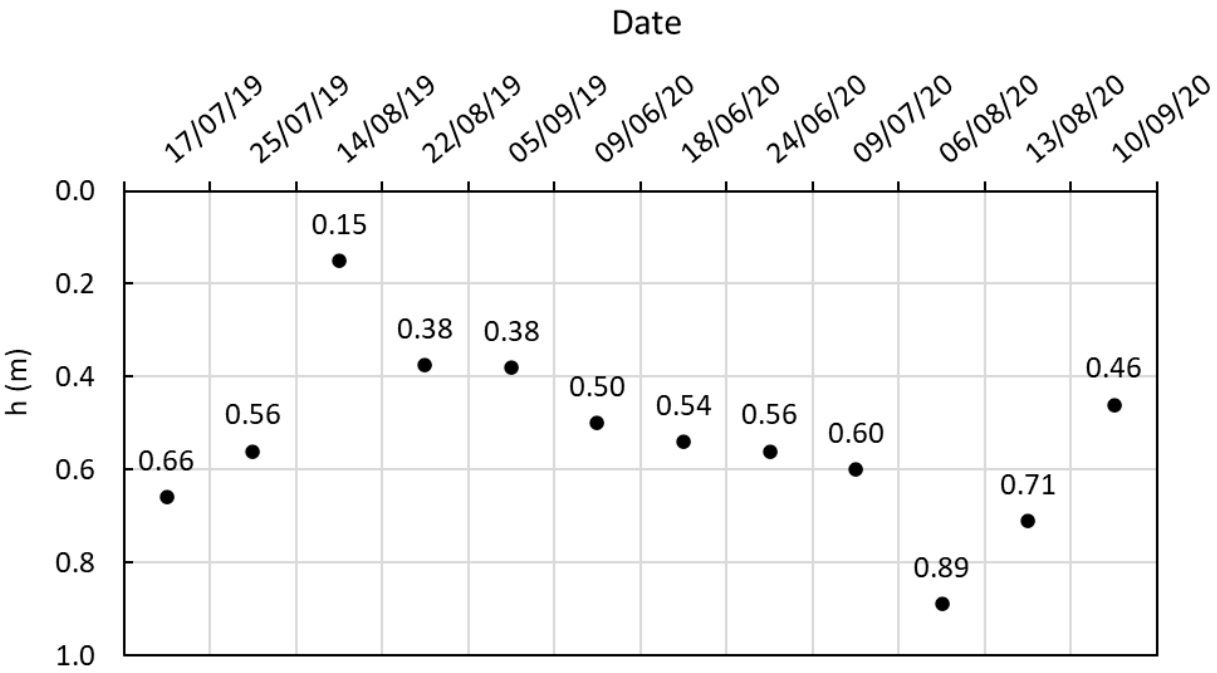


Figure 5. Groundwater table depth (h: depth below ground) measured during the 2019 and 2020 apple growing seasons.

Figure 6 and Table 3 present the soil moisture content (SMC) and electrical conductivity (EC) measurements taken during the 2019 and 2020 apple growing seasons, averaged across three measurement points at depths of 20, 30, and 50 cm. In 2019, at a 50 cm depth, the SMC ranged from 36% on 22 July to 44% on 14 August, with a decrease to 34% by 5 September. At a 30 cm depth, the SMC varied between 36% and 35%, and at a 20 cm depth, the moisture content was consistently lower, ranging from 26% to 29%. The EC values in 2019 at a 50 cm depth ranged from 3.2 dS m^{-1} on 22 July to 3.9 dS m^{-1} on 14 August, with an average of 3.4 dS m^{-1} across the season. At 30 cm, EC values ranged from 3.1 dS m^{-1} to 2.7 dS m^{-1}, and at 20 cm, EC ranged from 2.2 dS m^{-1} to 2.3 dS m^{-1}. In 2020, SMC levels at 50 cm showed a notable increase, peaking at 53% on 22 July, with the lowest value recorded at 34% on 9 July, resulting in an average of 47%. At 30 cm, moisture ranged from 34% to 42%, and at 20 cm, it fluctuated from 25% to 36%. EC at 50 cm in 2020 ranged from 3.2 dS m^{-1} on 18 June to 4.2 dS m^{-1} on 22 July, with an average of 3.5 dS m^{-1}. At 30 cm, EC varied from 2.9 dS m^{-1} to 3. dS m^{-1}, and at 20 cm, it ranged from 2.3 dS m^{-1} to 3.3 dS m^{-1}.

The data suggest that while SMC was relatively high, particularly at the 50 cm depth, the EC levels, particularly in 2020, approached or exceeded the 4.0 dS m^{-1} threshold that could potentially affect plant health, as this is the salinity threshold for many plant species [74]. However, despite fluctuations in both SMC and EC, the apple trees did not appear to experience significant water stress. Moisture levels in the deeper depths remained relatively stable, and no severe salinity conditions were observed. These findings suggest that the orchard was able to maintain adequate moisture levels for optimal growth, despite the varying environmental conditions across the two years. The low moisture observed

at the surface layer, particularly at 20 cm, is likely due to the permanent mulch applied, which helps reduce surface evaporation. As a result, moisture is retained in the deeper soil layers, where the apple tree root system primarily absorbs water, thereby benefiting from the moisture available at those depths.

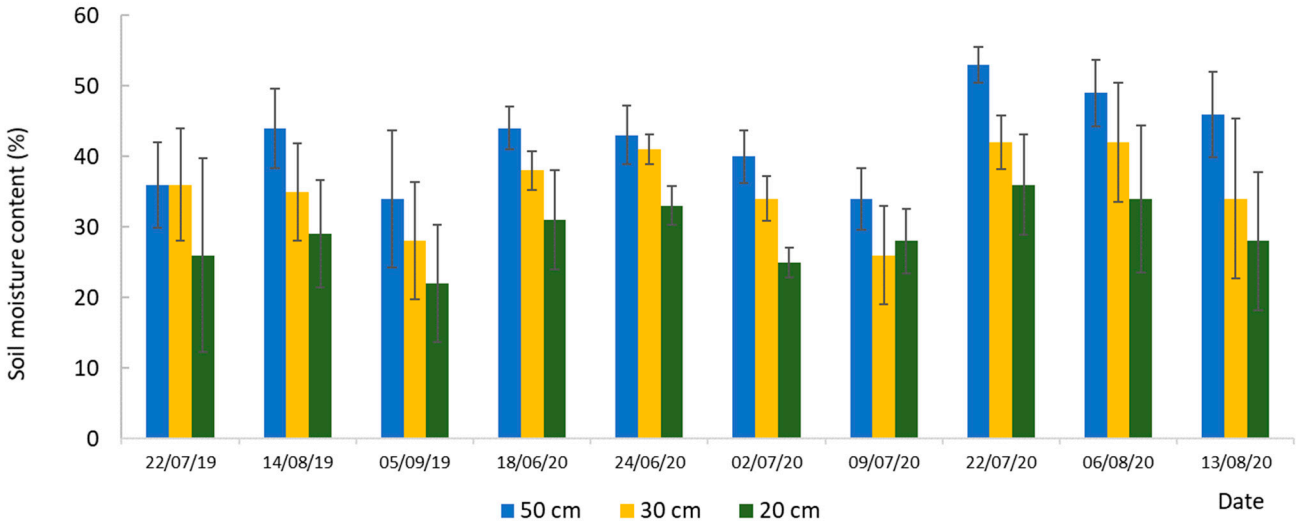


Figure 6. Average volumetric soil moisture content (% by volume) at depths of 20, 30, and 50 cm during the 2019 and 2020 growing seasons. Error bars indicate the variability in the measurements, represented by the standard deviation.

Table 3. Electrical conductivity (EC, in dS m^{-1}) measured at 50, 30, and 20 soil depths during the 2019 and 2020 apple growing seasons. Values are provided for specific measurement dates, with averages calculated for each depth across the seasons.

2019	**EC (dS m^{-1})**			**2020**	**EC (dS m^{-1})**		
	50 cm	30 cm	20 cm		50 cm	30 cm	20 cm
22 Jul.	3.2	3.1	2.2	18 Jun.	3.2	2.9	3.2
14 Aug.	3.9	2.7	2.4	24 Jun.	3.3	3.5	3.2
5 Sep.	3.0	2.7	2.3	02 Jul.	3.3	3.3	2.3
Average	3.4	2.8	2.3	09 Jul.	3.3	2.4	2.5
				22 Jul.	4.2	3.4	3.3
				06 Aug.	3.7	3.3	3.3
				13 Aug.	3.7	3.3	2.5
				Average	3.5	3.2	2.9

Soil available water content (AWC) was calculated relative to the field capacity and the permanent wilting point of each layer (Figure 7). The total AWC was 78.5 mm, while the available water in the soil water storage (AWS) ranged from 52.5 to 78.5 mm. The data indicate that AWS often fell below AWC, suggesting that the soil was not consistently at its maximum water capacity. In 2019, on 22 July, AWS was 66.5 mm, slightly below AWC, suggesting a relatively moist but not fully saturated soil. By 22 August, AWS had risen to 72.5 mm but still remained below AWC, suggesting stable yet suboptimal moisture levels. AWC dropped to 52.5 mm by 5 September, likely due to dry conditions or high plant water use. In 2020, AWC increased to 76.5 mm on 18 June, nearing AWS, and reached full saturation (78.5 mm) by 24 June. However, on 02 July, AWS declined to 64.5 mm, likely due to evaporation or plant uptake. AWC fluctuated slightly thereafter, reaching 78.5 mm on 22 July and 6 August, demonstrating maintained adequate soil moisture. On 13 August, AWC declined to 70.5 mm—still high, though lower than recent peaks. These observations

suggest that irrigation was effective, and there were good conditions for the hydric comfort of the crop, with no significant water deficit observed throughout the period.

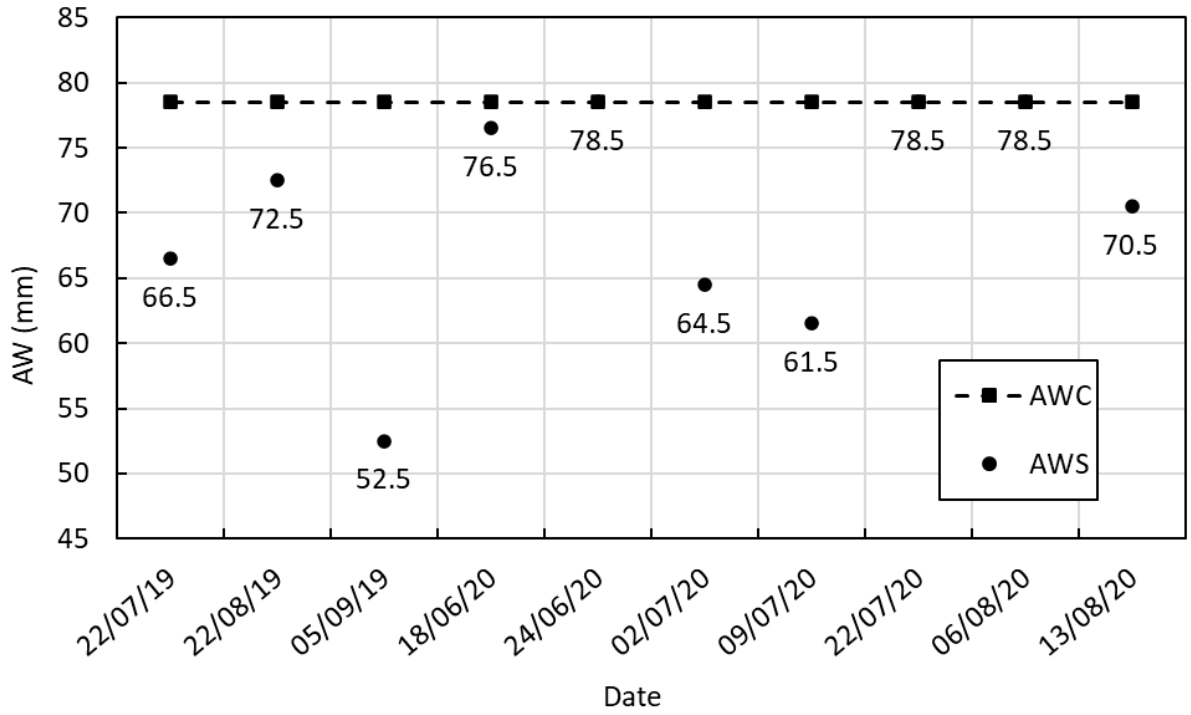


Figure 7. Observed total available water content (AWC) and available water storage (AWS) of the soil during the 2019 and 2020 seasons.

3.3. Crop Coefficients and Growing Period Stages

The K_c curve for apple orchards with permanent mulching, adapted from Tables 11 and 12 of FAO-56 [32], is illustrated in Figure 8. Given that the soil between the rows of the orchard is permanently covered, a K_c of 0.80 was derived from Table 12 after leaf drop during the period from November to mid-March. The length of the initial, development, mid-season, and end-season stages, as defined for deciduous orchards, were adapted from Table 11 and established as 20, 70, 105, and 35 days, respectively. These data were observed in the LVID, aligning with the standards set by FAO.

The growing period stages are also represented in Figure 8. During winter rest, in mid-autumn, the tree completely loses its foliage and enters a dormancy phase that lasts throughout the winter. In early spring, new leaves emerge, and flower buds develop, leading to the blooming of the apple trees. Successful pollination, primarily by bees, is crucial for fruit formation. At the end of spring and the beginning of summer, small apples begin to appear on the trees, with some being removed to allow the remaining fruits to grow larger and achieve optimal sizes. Throughout the summer, the fruits continue to increase in size, with critical nutrient and sugar accumulation influenced by temperature, humidity, and soil nutrition. Finally, at the end of summer and the beginning of autumn, the fruits reach ripeness and must be harvested for entry into the marketing circuit, typically occurring between mid-August and October, depending on the variety.

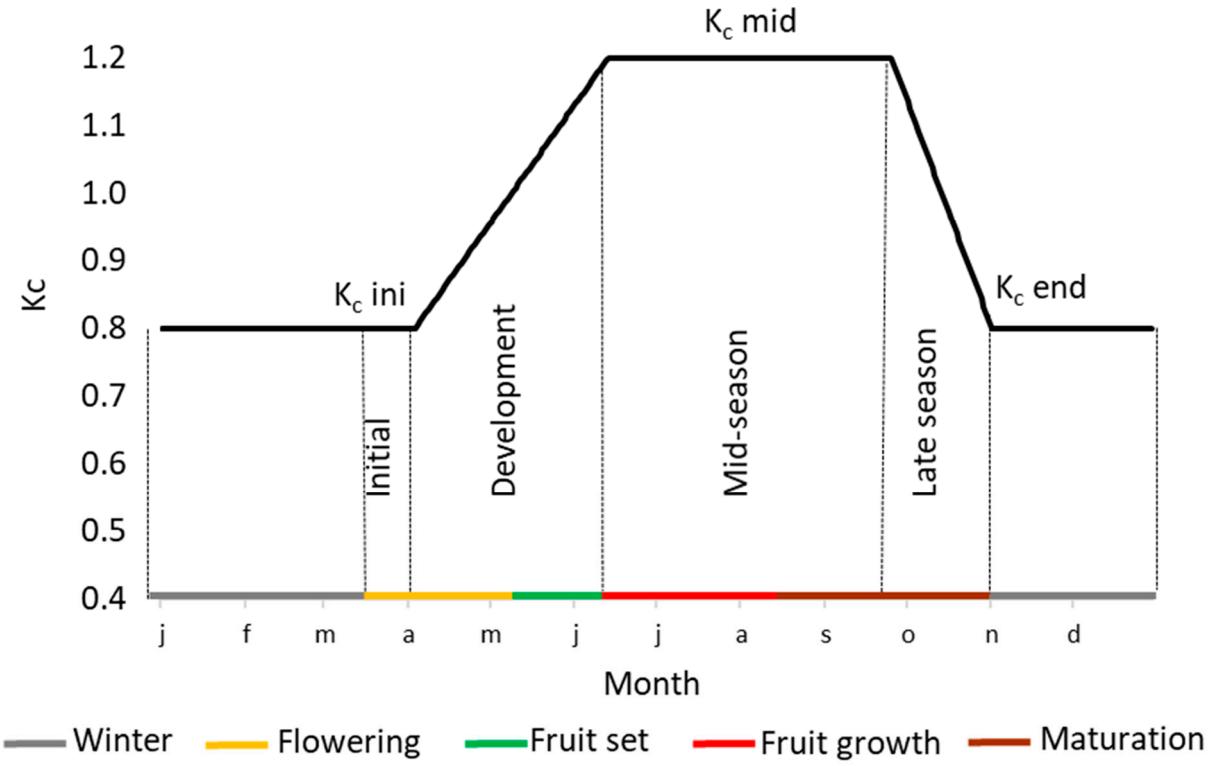


Figure 8. Crop coefficient curve for apple orchards with permanent mulching, showing the initial stage (Kc_{ini}), mid-season stage (Kc_{mid}), and end of the late season stage (Kc_{end}). The color bars represent the stages of the growing period.

3.4. Evapotranspiration and Crop Water Use

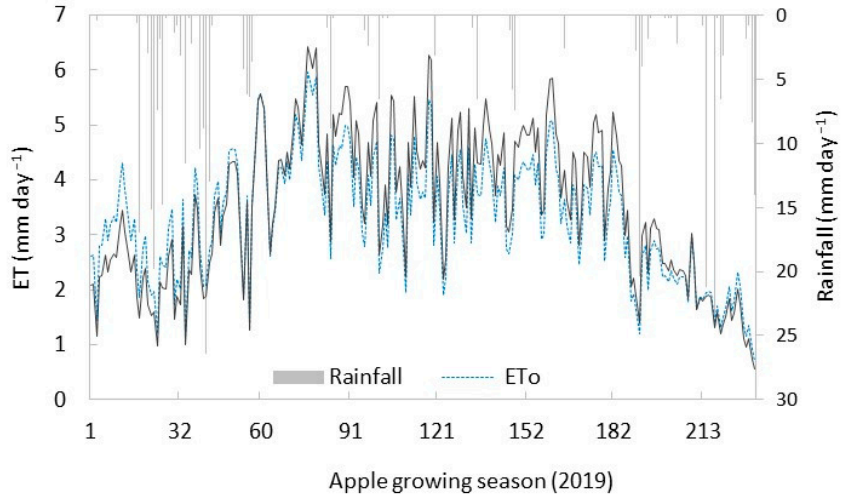
In orchards, ET is influenced by climatic factors, such as solar radiation, temperature, humidity, and wind speed, as well as the physiological characteristics of the trees. As shown in Table 4, for stages I and II, the highest evaporative demand was recorded in 2019, reflecting favorable weather conditions characterized by higher wind speed, temperature, and solar radiation, along with lower relative humidity, as detailed in Section 3.1. In contrast, stage III exhibited the greatest demand in 2020, while 2019 recorded lower values for this phase. Notably, stage IV experienced the highest evaporative demand in 2021, attributed to elevated temperatures and solar radiation during that period. Overall, ET values were highest in 2019, followed by 2020, with the lowest values observed in 2021. This variation highlights the significant impact of climatic factors on water demand throughout the apple-growing seasons.

The results regarding precipitation, evapotranspiration, and crop coefficients were consistent with the growth stages of the crop. Figure 9 illustrates the daily ET_o and ET_a, along with water input from rainfall for all growing seasons. The accumulated ET_o during the apple growing seasons was 766 766, 749, and 736 mm in 2019, 2020, and 2021, respectively. A higher average value of 3 mm day^{-1} was recorded in the early phase of 2019 compared to the corresponding periods in 2020 (2.1 mm day^{-1}) and 2021 (2.7 mm day^{-1}). This pattern continued into the development stage. In the middle stage, the average ET_o was higher in 2020. A significant decrease in evaporative demand was observed during the final phase, with values around 1.9 mm day^{-1} in both 2019 and 2020, and 2.1 mm day^{-1} in 2021.

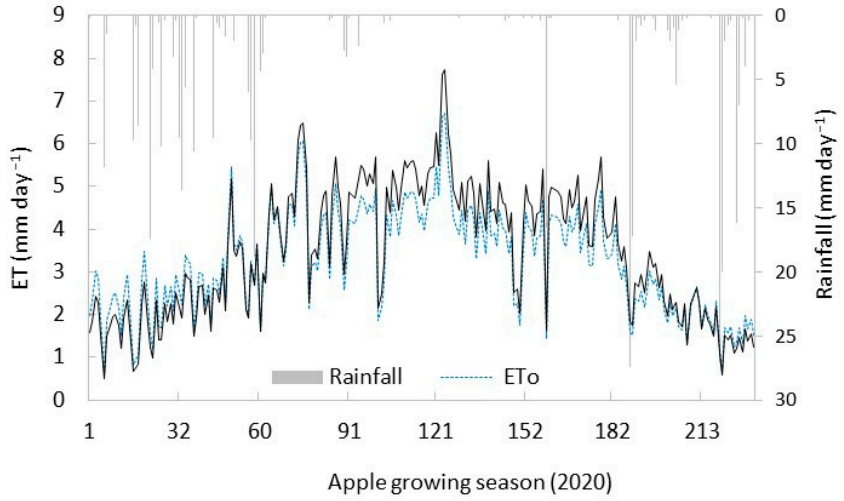
Table 4. Seasonal apple growth stages, irrigation (mm), precipitation (mm), reference evapotranspiration (ET_o), and apple crop evapotranspiration (ET_a) during the experimental seasons.

CGS	Irrigation (mm)				Precipitation (mm)				ET_o (mm) Daily (mm Day^{-1})				ET_o (mm) Period (mm)				Season CGS	ET_a (mm) Daily (mm Day^{-1})				ET_a (mm) Period (mm)			
	2019	2020	2021	Average	2019	2020	2021	Average	2019	2020	2021	Average	2019	2020	2021	Average		2019	2020	2021	Average	2019	2020	2021	Average
I	n.d.	n.d.	n.d.	---	18	32.6	7.6	19.4	3	2.1	2.7	2.6	60	42	53	52	I	2.4	1.7	2.1	2.1	48	33	43	41
II	n.d.	n.d.	n.d.	---	171.4	139.8	154.2	155.1	3.7	3.3	3.2	3.4	256	229	226	237	II	3.7	3.3	3.2	3.4	263	234	228	242
III	n.d.	n.d.	n.d.	---	67.6	70.6	92.2	76.8	3.6	3.9	3.6	3.7	380	410	382	391	III	4.2	4.5	4.2	4.3	456	492	458	469
IV	n.d.	n.d.	n.d.	---	83.4	91.2	116.2	96.9	1.9	1.9	2.1	2	70	68	75	71	IV	1.9	1.9	2.1	2.0	71	69	76	72
FCS	400	450	350	400	340.4	334.2	370.2	340	---	---	---	---	766	749	736	750	FCS	---	---	---	---	838	828	805	824

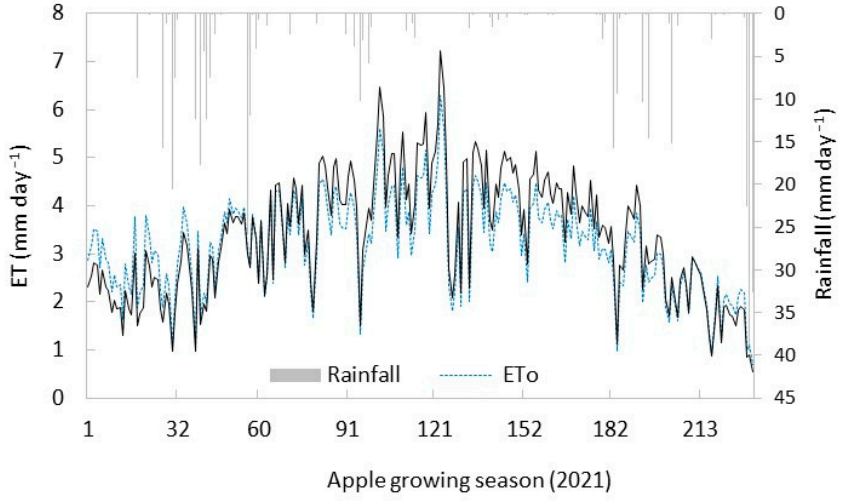
CGS—crop growth stage; FCS—full crop season; irrigation—total irrigation water during the season; precipitation—total precipitation for the three years in each stage, daily ET_o and ET_a are the average ET_o and ET_a values, respectively, for the period, and period ET_o and ET_a are the total accumulated values of ET_o and ET_a, respectively, for the period. Average represents the three-year average for precipitation, ET_o, and ET_a during the full crop season.



(**a**)



(**b**)



(**c**)

Figure 9. Daily ET_o and daily ET_a values calculated during the apple growing seasons of 2019 (**a**), 2020 (**b**), and 2021 (**c**) at the study site. Rainfall is represented by vertical bars.

According to the FAO-56 methodology and the recommended crop coefficients outlined in Section 2.3, the accumulated ET_a for the apple growing seasons was 838, 828, and

805 mm in 2019, 2020, and 2021, respectively. The ET_a values exceed those of ET_o due to the positive contribution from K_c. The transpiration component of the apple trees was minimal during the early stages (stage I) but increased significantly during the flowering and fruit-setting stages, primarily driven by the leaf surface area of the trees.

3.5. NDVI

Figure 10 shows the evolution of the NDVI processed by SPIDER and METRIC over the three study years, with field measurements overlaid for 2020. NDVI values outside the apple growing season were also considered to study the behavior of permanent mulching throughout the years. Overall, the three NDVI data sources show consistency across years, with values ranging from 0.40 to 0.79. The lowest values generally correspond to the mulch-cutting periods in January–February, May, and August, followed by rapid recovery, suggesting a resilient vegetation response. Despite winter dormancy and leaf loss, NDVI values remain around 0.55–0.60 due to the positive contribution of mulch. By mid-April, with spring rains and rising temperatures, the NDVI reaches 0.75–0.80, indicating a period of maximum vegetation vigor aligned with the active growth phase of the apple trees (stage II). During summer, values drop to 0.55–0.65 due to water stress on the unwatered mulch. After harvest, in October–November, the NDVI peaks again, likely due to autumn rains stimulating mulch growth and maintaining vegetation vigor despite leaf drop.

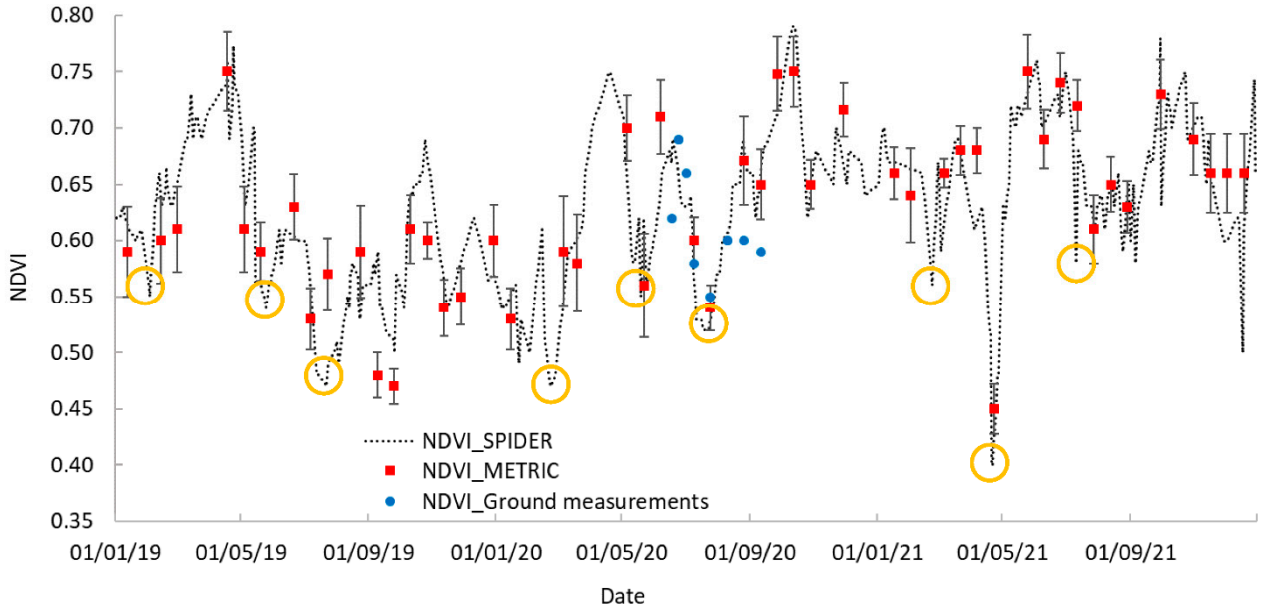


Figure 10. NDVI extracted from SPIDER (dotted lines for 2019, 2020, and 2021), ground field measurements (blue dots for 2020), and METRIC EEFlux (red squares for 2019, 2020, and 2021). Error bars represent the standard deviation on the 3 × 3-pixel averages from METRIC. Yellow circles represent the cutting events for the living mulch, highlighting the timing of each intervention.

NDVI_METRIC generally aligns with NDVI_SPIDER, though slight differences occur, either higher or lower in some instances. This discrepancy may stem from the different spatial resolutions: EEFlux images have a 30 m resolution, compared to the 10–20 m resolution of SPIDER's Sentinel-2 images. Ground measurements between July and September 2020 closely match NDVI_SPIDER values, validating the accuracy of automatic measurements for this period. However, slight variations may arise from local site conditions and measurement adjustments due to tree height, even with the use of the extender.

Figure 11 presents the NDVI map derived from the drone flight imagery, visually highlighting the distinction between the apple trees and the inter-row grass cover. The

analysis confirmed a significant difference in NDVI values. Apple trees exhibited a mean NDVI of 0.75 (±0.07), while the inter-row grass cover had a mean NDVI of 0.50 (±0.05). These values illustrate the contrasting characteristics of the two vegetative components. The higher NDVI of the apple trees reflects their greater photosynthetic activity, consistent with their role as the primary productive vegetation. In contrast, the lower NDVI of the inter-row grass cover can be attributed to its function as soil cover, which is subject to hydric stress and less vigorous growth.

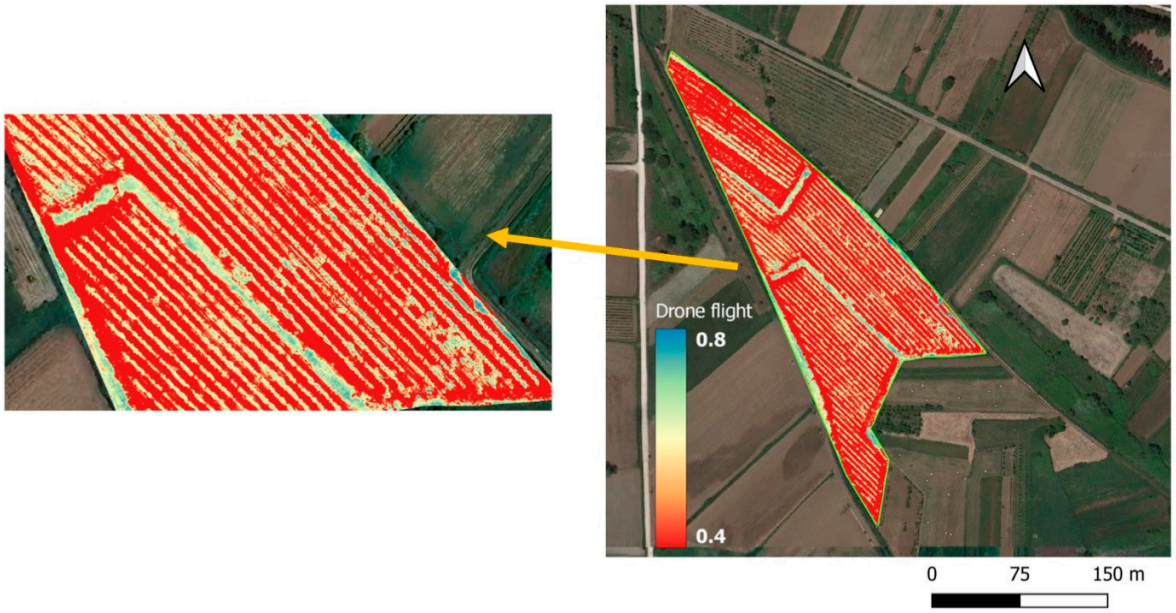


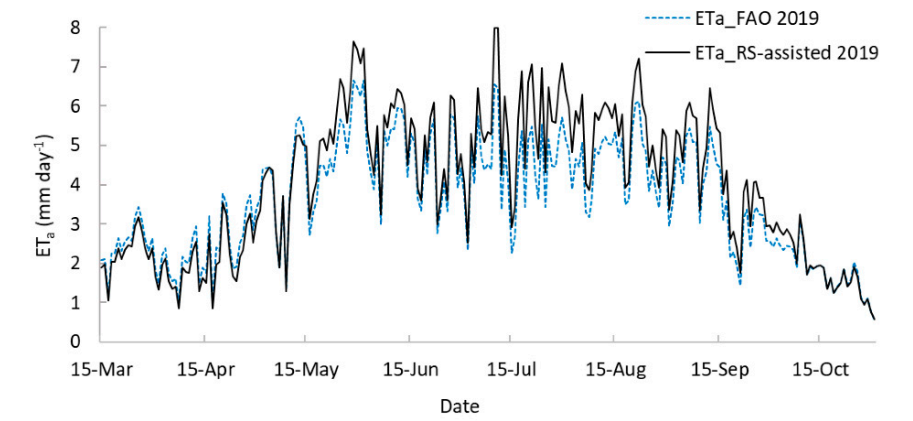
Figure 11. The NDVI processed from the drone flight conducted on 26 July 2021.

3.6. Calibration of the RS-Assisted Kc-NDVI Relationship

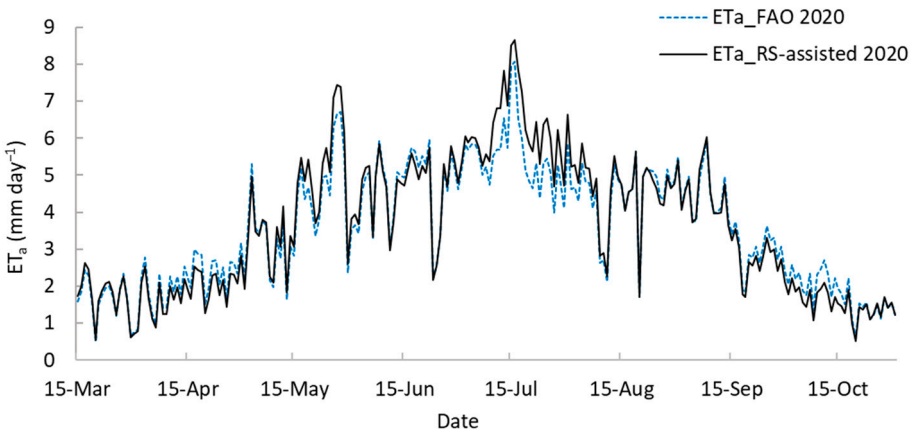
Figure 10 demonstrates variability in apple conditions across different years, effectively captured by NDVI data from satellites. However, the FAO-56 methodology for deriving ET_a does not account for this variability, as it assigs the same crop coefficients to all surface conditions. Here, we present a method that utilizes a calibrated equation, $K_c = K_c$ (NDVI), specifically tailored to the unique conditions of our apple orchard. This approach utilizes a temporal series of satellite images to reproduce a range of crop conditions under different management practices, leading to diverse ET_a values. This methodology embodies the well-known RS-assisted FAO-56 approach, which has been successfully applied to various crops, though it is rarely seen in apple orchards.

Using data from 2019, a year characterized by typical meteorological conditions, effective vegetation management, and optimal crop yield, K_c was parametrized as a linear function of the NDVI: $K_c = -1.6243(\text{NDVI}) + 2.0576$. A strong correlation was observed between apple K_c and the NDVI during different growth stages, with an R^2 value of 0.75.

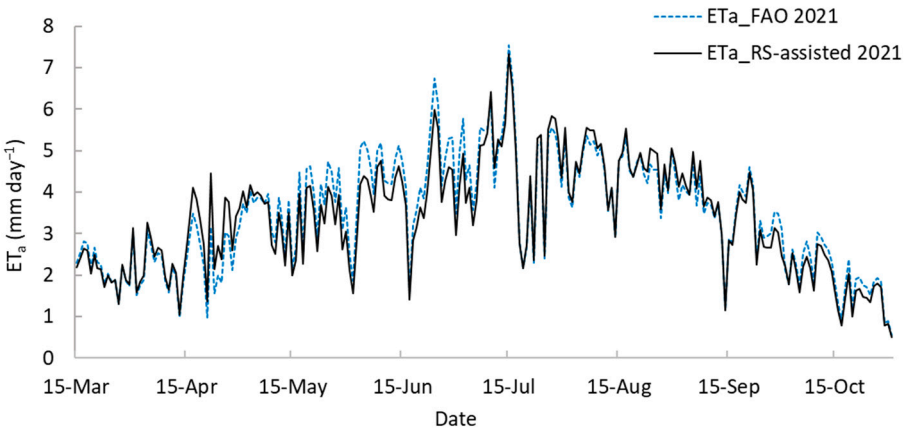
The K_c values suggested by FAO-56 for the three crop seasons were replaced with those obtained from the $K_c = K_c$ (NDVI) equations. Subsequently, ET_a was recalculated for the entire dataset to highlight the impact of this RS method on the variability of the results. The findings are presented in Figure 12, which illustrates a strong correspondence among the results for all three seasons.



(**a**)



(**b**)



(**c**)

Figure 12. ET_a from RS-assisted FAO-56 evolution compared with ET_a from the traditional FAO-56 method during the apple growing seasons of 2019 (**a**), 2020 (**b**), and 2021 (**c**) at the study site.

3.7. Assessment of ET_a from RS-Assisted FAO-56

The assessment of independent ET_a values provided by the METRIC surface energy balance model was conducted to validate the RS-assisted FAO-56 technique. The maps in Figure 13 show two examples of the spatial distributions of ET_a derived from both the METRIC and RS-assisted FAO-56 approaches.

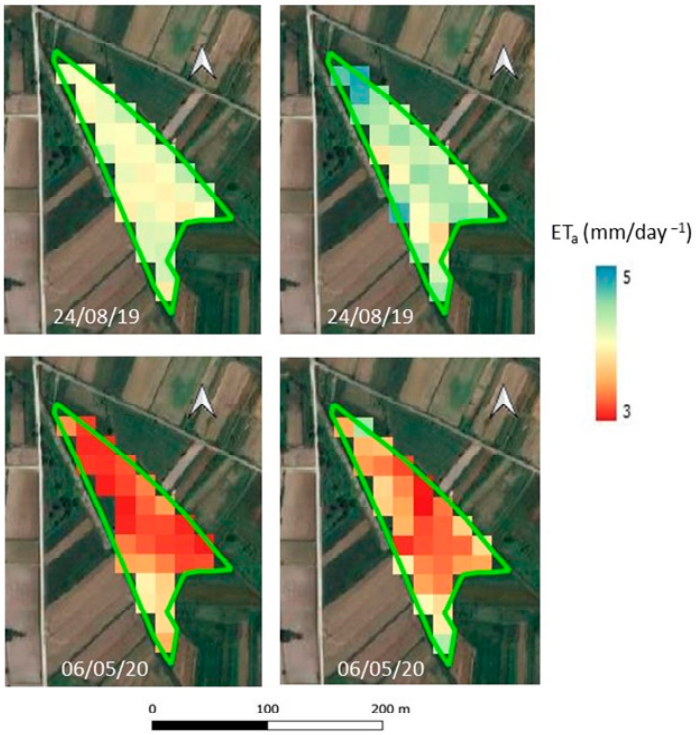


Figure 13. Examples of ET_a maps obtained from the METRIC (**left**) and the RS-assisted FAO-56 approach (**right**) for two different dates: 24 August 2019 (**upper**) and 6 May 2020 (**lower**). The apple orchard is outlined in green.

Figure 14 shows a comparison of daily ET_a values estimated from both methodologies for dates with available Landsat 8 images across the three campaigns. The availability of satellite images was limited due to the characteristic cloudiness of the LVID and the 16-day temporal resolution of Landsat 8.

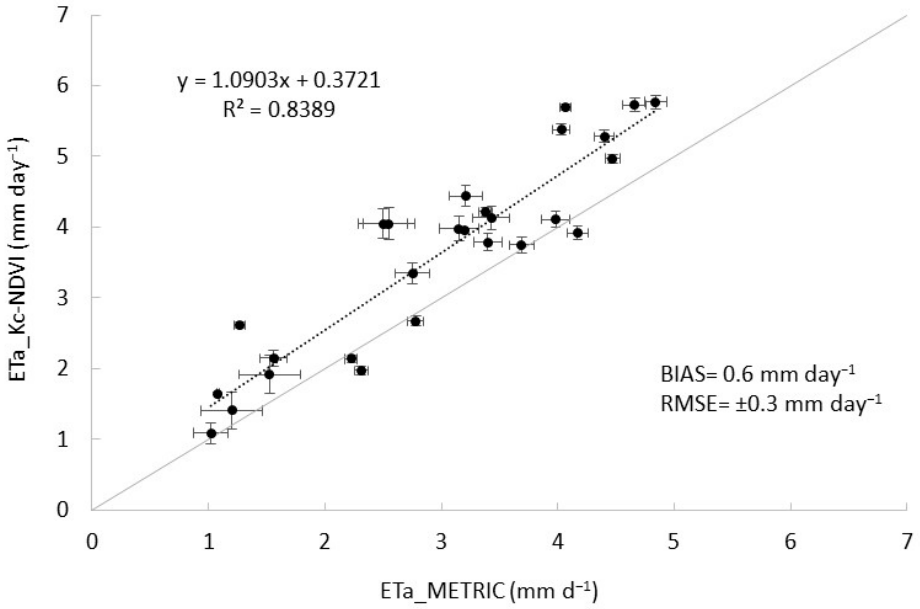


Figure 14. Linear regression between mean ET_a values provided by METRIC and ET_a calculated from the derived $K_c = K_c(NDVI)$ relationship. The dotted line represents the linear regression. The gray line represents the 1:1 relationship, included as a reference to evaluate the agreement between observed and estimated values. Error bars indicate spatial variability, representing the standard deviation of ET_a values from METRIC on the *x*-axis and ET_a resulting from the $K_c = K_c(NDVI)$ approach on the *y*-axis.

3.8. Crop Yield and Water Productivity

Table 5 presents the contrast between the RS-assisted ET_a values and those obtained using the FAO-56 method to assess the differences between the two approaches, as well as the corresponding data for Y, WP, and WUE across the three experimental years. In 2019, the RS-assisted ET_a was 10.4% higher than the FAO-56 estimate, while in 2020, it showed a 2.0% increase. In 2021, however, the RS-assisted ET_a was 2.5% lower than the FAO-56 estimate. On average, the RS-assisted ET_a was 3.3% higher than the FAO-56 values over the three years. These variations reflect differences in the methods used for estimating crop water requirements, with the RS-assisted approach potentially accounting for site-specific factors, such as vegetation cover and real-time climate data.

Table 5. Analysis of the variation in apple ET_a (FAO-56 vs. RS assisted), yield, water productivity, and water use efficiency across the 2019–2021 experimental seasons.

Apple Crop Season	ET_a FAO-56 (mm)	ET_a RS-A (mm)	Var. ET_a (%)	Y (t ha^{-1})	WP (kg m^{-3})	WUE FAO-56 (kg m^{-3})	WUE RS-A (kg m^{-3})	Var. WUE (%)
2019	838	925	+10.4	32 ± 2.5	4.32	1.13	1.25	+10.6
2020	828	845	+2.0	24 ± 3.8	3.06	1.06	1.08	+1.9
2021	805	785	−2.5	33 ± 3.1	4.58	1.12	1.09	−2.7
Average	824	852	+3.3	30	3.99	1.10	1.14	+3.6

Y—yield (total apple production with a corresponding standard deviation, t ha^{-1}); WP—water productivity (Y(tha $^{-1}$)/(I + P, m^3 ha^{-1}), kg m^{-3}); WUE—water use efficiency: ET_a (mm)/(I + P, m^3 ha^{-1}), kg m^{-3}. The 3-year average values were also calculated.

The highest yield was recorded in 2021 at 33 ± 3 t ha^{-1}, and the lowest in was 2020 at 24 ± 4 t ha^{-1}, with an average yield of 30 t ha^{-1} across the three seasons. WP was the highest in 2021 at 4.58 kg m^{-3} compared to 4.32 kg m^{-3} in 2019 and 3.06 kg m^{-3} in 2020. WUE RS-assisted values were the highest in 2019 at 1.25 kg m^{-3}, followed by 1.08 kg m^{-3} in 2020 and 1.09 kg m^{-3} in 2021, with a variation of +10.6%, +1.9%, and −2.7%, respectively, compared to WUE according to ET_a calculated from FAO-56. The average WUE over the three years was 1.14 kg m^{-3}, with a variation of +3.6%.

The annual variations in WP and WUE can be attributed to fluctuations in apple production during the 2019–2021 seasons. In 2019, apple production increased by 35%, benefiting from favorable weather during the flowering and fruit-setting stages, along with timely irrigation to offset low rainfall [71]. Conversely, in 2020, production fell by 25% due to adverse weather conditions and physiological constraints during these critical growth phases, compounded by hailstorms and sunscalds that negatively affected fruit quality [72]. In 2021, production rebounded with a 30% increase, particularly in the Oeste region. Forecasts indicated a 10% increase for Gala varieties and a 30% increase for Fuji group varieties, driven by favorable conditions during crucial growth phases [73].

4. Discussion

4.1. Evapotranspiration and Irrigation Water Applied

The research conducted, which included monitoring the irrigation system, soil moisture levels, and crop development, particularly the growth of permanent mulch, provided valuable insights into the agroecosystem of apple orchards, especially regarding water management. This knowledge aligns with findings from other studies, highlighting that modern apple orchards are significant consumers of water resources and have specific needs, including (i) a high water requirement, in which apple trees generally need a substantial amount of water, especially during flowering and fruit-setting stages, with demand largely influenced by climate, soil type, and management practices [75], and (ii) evapotranspiration, in which apple trees exhibit high evapotranspiration rates, particularly in hot, dry climates. This results in significant water loss through both leaf transpiration and

soil evaporation, highlighting the importance of using LM to conserve soil moisture [76]. (iii) The impact of water on production involves water availability directly influencing both the quality and quantity of apple production. Insufficient water often leads to smaller, lower-quality fruits [77]. (iv) Irrigation management is the idea that effective irrigation management is essential for maximizing production in apple orchards. Efficient systems, like drip irrigation, are commonly employed to ensure that plants receive the necessary moisture [78]. Therefore, apple cultivation requires special attention to irrigation and water management, especially in regions where water availability is limited.

In our study, the measured apple ET_a ranged between 805 and 838 mm for the full crop season. Cao et al. reported ET_a values between 415 mm and 989 mm in an arid region in China (orchard without LM) [79]. Other studies, also without LM, using sap flow and micro-lysimeter methods estimated ET_a rates between 583 and 674 mm [80]. Specially, focusing on July, a study from Rubauskis in Latvia presented an evapotranspiration rate of 5.3 mm day^{-1}, which aligns with our findings for the same month (4.52, 5.51, and 4.77 mm day^{-1} for 2019, 2020, and 2021, respectively), in an orchard with LM [81]. Another study from Spain, with LM, reported mean daily ET_a values during midseason of 3.24 and 3.77 mm day^{-1} over two years, consistent with our results (4.2, 4.5, and 4.2 mm day^{-1} for 2019, 2020, and 2021, respectively) [82].

In general, the amount of irrigation water used in agriculture raises concerns about water as a limited resource, both in terms of quality and quantity. Major issues include (i) water scarcity in several areas exacerbated by droughts and the consequent deterioration of water quality; (ii) soil salinization and pollution, which have led to water policies promoting the rational use of this resource; and (iii) the effects of climate change [83]. In our study, the irrigation water applied across the three seasons varied between 350 and 450 mm, aligning with other studies that report similar irrigation requirements of 400–500 mm [80].

4.2. Crop Coefficient

In previous works, Allen et al. [32] reported that apple trees in active ground cover under frost-free conditions had standardized Kc values corrected for typical environmental conditions (RH_{min} = 45% and u_2 = 2 m s^{-1}) of K_{Cini} = 0.80, K_{Cmid} = 1.20, and K_{Cend} = 0.85, with values dropping to 0.50–0.80 after leaf drop.

During the initial phase (Phase I), FAO-56 recommends a constant K_c of 0.80. However, our RS-assisted approach revealed higher values (0.91, 1.02, and 0.99 in 2019, 2020, and 2021, respectively). These increased values are likely attributable to vigorous mulch growth, enhanced by early spring rains, which improved soil moisture retention and the microclimate, thereby boosting evapotranspiration rates and, consequently, K_c values. This finding aligns with other studies suggesting that mulch positively impacts K_c, particularly when early rains enhance soil moisture availability [75].

In the development phase (Phase II), FAO-56 suggests a gradual increase in K_c from 0.80 to 1.20, reflecting the growing water needs of plants. Our approach demonstrated deviations from these FAO values, influenced by management practices, such as mulch cutting. In 2019, RS-assisted K_c values temporarily dropped below the FAO value in May but recovered after the cutting event. A similar trend occurred in 2020, with lower values observed in late May. In 2021, RS-assisted K_c values remained higher than the FAO's until May 8, after which they aligned more closely with the FAO recommendations. These fluctuations underscored the combined impact of management practices and environmental factors on evapotranspiration rates.

In mid-season (Phase III), FAO-56 recommends a constant K_c of 1.20. Our study, however, recorded variations in RS-assisted K_c values: 1.17, 1.04, and 0.99 in 2019, 2020, and

2021, respectively, largely influenced by the mulch cut before harvest. Studies estimating K_c in apple orchards have reported values ranging from 1.11 to 1.43 for the middle season [79].

In the late phase (Phase IV), FAO-56 K_c values decrease from 1.20 to 0.85 (average 1.02), while other studies repost values ranging from 1.09 to 1.22 for the late season [84]. Our study, however, found different trends in average RS-assisted values (1.04 in 2019, very close to the FAO value; 0.89 in 2020; and 0.90 in 2021), possibly reflecting the influence of specific climate conditions during these periods.

These variations demonstrate that while FAO K_c values provide a standard, the actual K_c can fluctuate based on local conditions, crop management, and environmental factors. RS data, especially when combined with local water management practices, provide a valuable tool for more accurate monitoring and estimation of crop water needs. This is evident in studies using RS for irrigation management in Spain ([58,60]) and other regions [85].

4.3. Water Productivity and Crop Yield

Research indicates that the WP in apple orchards can reach up to 4.45 kg m^{-3}, as noted by Cao [79]. Our study's findings, which report an average WP of 3.99 kg m^{-3} over three seasons, align with these earlier observations. Enhancing WP involves two key strategies: (i) increasing water use efficiency by minimizing applied water without compromising yields and (ii) elevating productivity by boosting crop yields while maintaining current water usage levels. On a broader scale, where water conservation is paramount, the first approach is generally favored, as it seeks to reduce water consumption while ensuring food production [86]. If the goal is to cut back on water usage, it is crucial to encourage farmers to adopt water-saving practices. However, many farmers, especially those facing economic challenges, often prioritize maximizing yield over optimizing water usage, a trend highlighted by Pouladi et al. [87]. This issue is particularly pressing in the LVID region, where water consumption for members of WUAs is determined by plot size rather than actual usage, leading to inefficient and sometimes irrational water management. Recent rehabilitation efforts, initiated in 2021 under Portugal's National Irrigation Programme, aim to address these challenges [88]. The program focuses on modernizing irrigation infrastructure by transitioning to pressure pipe systems and incorporating meters for better monitoring of water use.

4.4. Management of Permanent Living Mulch

In this study, LM was not irrigated, allowing for a focus on sustainable, eco-friendly practices that conserve water and enhance soil health [75]. Without increasing water demand, LM aligns with strategies for water conservation, soil improvement, and biodiversity promotion, fostering resilient agricultural systems and improving water use efficiency.

While LM in apple orchards offers several advantages, careful management is required to prevent competition with trees for water and nutrients, which can potentially affect yield [89]. Effective strategies to mitigate this competition include selecting species with robust growth for weed suppression, shallow roots to minimize interference with trees, compact size to prevent shading, and perennial life cycles to ensure year-round cover. Regular mowing and thoughtful species selection also help balance the benefits of LM with the needs of the crop.

Mechanical techniques, such as strip tillage and root pruning, can further enhance the performance of LM performance without causing excessive soil disturbance. Recent studies have suggested that combining mechanical and reduced chemical controls (e.g., herbicide application) can optimize weed management and crop yield. This approach has

shown promise in crops like tomatoes and cabbage, where LM contributes to increased biomass and improved nitrogen uptake [90,91].

Furthermore, while LM can attract beneficial organisms, it may also harbor pests and invasive weeds. To mitigate these risks, it is advisable to choose pest-resistant plant species and implement integrated pest management strategies. The practices can help create a sustainable orchard environment.

4.5. Potential and Challenges of RS for Improving Crop Management

RS technology offers significant potential to improve apple orchard management by providing near-continuous spatial information on various aspects of crop health and environmental conditions. These data allow for more precise management in areas such as fertilization, pest control, and irrigation. Drone imagery, for example, provides high spatial resolution data that capture the evapotranspiration contributions from apple trees and mulch, offering an enhanced understanding of water use efficiency and crop development. When integrated with satellite imagery, these data enrich the satellite information, offering a more detailed picture of the orchard's health and needs. One of the key advantages of RS is its ability to refine irrigation management. Adjusting irrigation schedules based on real-time crop and environmental data enables the transition to precision irrigation, optimizing water use and improving efficiency.

Furthermore, RS technologies can help assess the performance of mulch by correlating it with environmental functions, such as water retention and temperature regulation, thus optimizing the effectiveness of agroecosystems. A relevant example of the potential impact of this approach is the ECOPOMAR project, launched in 2024 by the Association of Apple Producers of Alcobaça [92]. This project promotes sustainability in apple orchards through integrated pest management without the use of chemicals, rainwater retention via lagoons and drainage systems, and carbon sequestration. Additionally, ECOPOMAR focuses on producing apples based on quality and flavor rather than market competitiveness.

5. Conclusions

This study aimed to estimate the water requirements in drip-irrigated apple orchards using the FAO-56 methodology for ET_a estimation, complemented by satellite-based RS. Strong correlations were found between the FAO K_c values and the NDVI evolution, with an R^2 of 0.75. The RS-assisted method was compared to the METRIC model, showing a small average estimation error of ± 0.3 mm day^{-1} with a low bias of 0.6 mm day^{-1}. These results demonstrate the potential of the RS method for monitoring ET_a, improving water productivity, and predicting crop yield, offering a practical tool for farmers. Additionally, the method can support water managers in large-scale irrigation networks. Future research should address the challenges of cloud cover and the spatial resolution of Landsat images, exploring high-resolution platforms, such as PlanetScope. Further work is also needed to apply the $K_c = K_c(NDVI)$ equation to other apple-growing regions and areas with bare soil.

Author Contributions: J.M.S. and J.M.G. conceptualized and designed the study; S.F., J.M.G., R.E. and H.D. performed the field observations; S.F., J.M.S. and J.M.G. analyzed and validated the data; S.F. wrote the paper with contributions from the other authors. All authors have read and agreed to the published version of the manuscript.

Funding: This research was funded by the Portuguese Foundation for Science and Technology, grant number 2020.07088.BD; Program PDR2020, co-funded by FEDER under the Innovation Measure, Portugal, grant number PDR2020-1.0.1-FEADER-030911; and the Education, Culture and Sports Council, JCCM, Spain, grant number SBPLY/21/180501/000070, together with FEDER.

Data Availability Statement: The data presented in this study are available upon request from the corresponding author.

Acknowledgments: The authors would like to thank the Lis Valley Water User's Association and Vítor Duarte for their collaboration during the measuring campaigns. Special thanks are also extended to Antonio Molina for processing the UAV flight data.

Conflicts of Interest: The authors declare no conflicts of interest.

References

1. FAOSTAT. Available online: http://www.fao.org/faostat/en/#data/QC/visualize (accessed on 15 September 2024).
2. INE. *Agricultural Statistics*; INE: Lisbon, Portugal, 2021. Available online: https://www.ine.pt/xportal/xmain?xpid=INE&xpgid=ine_publicacoes&PUBLICACOESpub_boui=439500127&PUBLICACOESmodo=2 (accessed on 11 October 2024).
3. APMA. Specifications—Alcobaça Apple. 2014. Available online: https://tradicional.dgadr.gov.pt/images/prod_imagens/frescos/docs/CE_maca_alcoba%C3%A7a_2021.pdf (accessed on 15 September 2024).
4. Paušič, A.; Tojnko, S.; Lešnik, M. Permanent, undisturbed, in-row living mulch: A realistic option to replace glyphosate-dominated chemical weed control in intensive pear orchards. *Agric. Ecosyst. Environ.* **2021**, *318*, 107502. [CrossRef]
5. Tu, A.; Xie, S.; Zheng, H.; Li, H.; Li, Y.; Mo, M. Long-term effects of living grass mulching on soil and water conservation and fruit yield of citrus orchard in south China. *Agric. Water Manag.* **2021**, *252*, 106897. [CrossRef]
6. Hartwig, N.L.; Ammon, H.U. Cover crops and living mulches. *Weed Sci.* **2002**, *50*, 688–699. [CrossRef]
7. Cougnon, M.; Durand, J.-L.; Julier, B.; Barre, P.; Litrico, I. Using perennial plant varieties for use as living mulch for winter cereals: A review. *Agron. Sustain. Dev.* **2022**, *42*, 110. [CrossRef]
8. Brunetto, G.; Oliveira, B.S.; Ambrosini, V.G.; Couto, R.D.R.; Sete, P.B.; dos Santos Junior, E.; Loss, A.; Stefanello da Silva, L.O.; Gatiboni, L.C. Nitrogen availability in an apple orchard with weed management. *Cienc. Rural* **2018**, *48*. [CrossRef]
9. Granatstein, D.; Sanchez, E. Research knowledge and needs for orchard floor management in organic tree fruit systems. *Int. J. Fruit Sci.* **2009**, *9*, 257–281. [CrossRef]
10. Zhao, L.; Liu, Y.; Zhao, W. Effects of Living Mulch on Soil Nutrient Leaching and Soil Erosion in Agroecosystems. *J. Environ. Manag.* **2020**, *256*, 109963.
11. Polverigiani, S.; Franzina, M.; Neri, D. Effect of soil condition on apple root development and plant resilience in intensive orchards. *Appl. Soil Ecol.* **2018**, *123*, 787–792. [CrossRef]
12. Tang, M.; Gao, X.; Wu, P.; Li, H.; Zhang, C. Effects of Living Mulch and Branches Mulching on Soil Moisture, Temperature and Growth of Rain-Fed Jujube Trees. *Plants* **2022**, *11*, 2654. [CrossRef]
13. Teasdale, J.R. Contribution of cover crops to weed management in sustainable agricultural systems. *J. Prod. Agric.* **1996**, *9*, 475–479. [CrossRef]
14. Balmer, O.; Pfiffner, L.; Schied, J.; Willareth, M.; Leimgruber, A.; Luka, H.; Traugott, M. Noncrop flowering plants restore top-down herbivore control in agricultural fields. *Ecol. Evol.* **2013**, *3*, 2634–2646. [CrossRef]
15. Simon, S.; Lesueur-Jannoyer, M.; Plénet, D.; Lauri, P.-É.; Le Bellec, F. Methodology to design agroecological orchards: Learnings from on-station and on-farm experiences. *Eur. J. Agron.* **2017**, *82*, 320–330. [CrossRef]
16. Lipecki, J. Weeds in orchards—Pros and contras. *J. Fruit Ornam. Plant Res.* **2006**, *14*, 13–18.
17. Yvoz, S.; Cordeau, S.; Ploteau, A.; Petit, S. A framework to estimate the contribution of weeds to the delivery of ecosystem (dis)services in agricultural landscapes. *Ecol. Indic.* **2021**, *132*, 108321. [CrossRef]
18. Hammermeister, A.M. Organic Weed Management in Perennial Fruits. *Sci. Hortic.* **2016**, *208*, 28–42. [CrossRef]
19. Licznar-Małańczuk, M. Occurrence of Weeds in an Orchard Due to Cultivation of Long-Term Perennial Living Mulches. *Acta Agrobot.* **2020**, *73*, 7326. [CrossRef]
20. European Commission. Common Agricultural Policy. Available online: https://agriculture.ec.europa.eu/common-agricultural-policy/income-support/greening_en (accessed on 11 May 2024).
21. Sha, J.; Wang, F.; Xu, X.; Chen, Q.; Zhu, Z.; Jiang, Y.; Ge, S. Studies on the translocation characteristics of ^{13}C-photoassimilates to fruit during the fruit development stage in 'Fuji' apple. *Plant Physiol. Biochem.* **2020**, *154*, 636–645. [CrossRef]
22. Lanauskas, J.; Kviklys, D.; Kviklienė, N.; Uselis, N.; Viškelis, P.; Rubauskis, E. Effect of Soil Management on Tree Nutrition and Yield in Apple Organic Orchards. *Acta Hortic.* **2014**, *1058*, 175–180. [CrossRef]
23. Chen, Y.; Wen, X.; Sun, Y.; Zhang, J.; Wu, W.; Liao, Y. Mulching practices altered soil bacterial community structure and improved orchard productivity and apple quality after five growing seasons. *Sci. Hortic.* **2014**, *172*, 248–257. [CrossRef]
24. Ren, J.; Li, F.; Yin, C. Orchard grass safeguards development of fruit industry in China. *J. Clean. Prod.* **2023**, *382*, 135291. [CrossRef]
25. Han, S.; Zhao, J.; Liu, Y.; Xi, L.; Liao, J.; Liu, X.; Su, G. Effects of green manure planting mode on the quality of Korla fragrant pears (*Pyrus sinkiangensis* Yu). *Front. Plant Sci.* **2022**, *13*, 1027595. [CrossRef] [PubMed]

26. Fu, X.; Liu, J.; Huang, W. Effects of natural grass on soil microbiology, nutrient and fruit quality of Nanfeng tangerine yard. *Acta Hortic. Sin.* **2015**, *49*, 1404–1414.
27. Muscas, E.; Cocco, A.; Mercenaro, L.; Cabras, M.; Lentini, A.; Porqueddu, C.; Nieddu, G. Effects of vineyard floor cover crops on grapevine vigor, yield, and fruit quality and the development of the vine mealybug under a Mediterranean climate. *Agric. Ecosyst. Environ.* **2017**, *237*, 203–212. [CrossRef]
28. Goyal, S.; Mishra, M.M.; Hooda, I.S.; Singh, R. Organic matter-microbial biomass relationships in field experiments under tropical conditions: Effects of inorganic fertilization and organic amendments. *Soil Biol. Biochem.* **1992**, *24*, 1081–1084. [CrossRef]
29. Bałuszyńska, U.B.; Rowińska, M.; Licznar-Małańczuk, M. Grass Species as Living Mulches—Comparison of Weed Populations and Their Biodiversity in Apple Tree Rows and Tractor Alleys. *Acta Agrobot.* **2022**, *75*, 758. [CrossRef]
30. Graham, P.H.; Vance, C.P. Legumes: Importance and Constraints to Greater Use. *Plant Physiol.* **2003**, *131*, 872–877. [CrossRef] [PubMed]
31. Luo, Y.; Ma, L.; Feng, Q.; Luo, H.; Chen, C.; Wang, S.; Yuan, Y.; Liu, C.; Cao, X.; Li, N. Influence and Role of Fungi, Bacteria, and Mixed Microbial Populations on Phosphorus Acquisition in Plants. *Agriculture* **2024**, *14*, 358. [CrossRef]
32. Allen, R.G.; Pereira, L.S.; Raes, D.; Smith, M. *Crop Evapotranspiration—Guidelines for Computing Crop Water Requirements*; FAO Irrigation and Drainage Paper No. 56; Food and Agriculture Organization: Rome, Italy, 1998; ISBN 92-5-104219-5.
33. Yang, Y.; Feng, Z.; Huang, H.Q.; Lin, Y. Climate-Induced Changes in Crop Water Balance during 1960–2001 in Northwest China. *Agric. Ecosyst. Environ.* **2008**, *127*, 107–118. [CrossRef]
34. Girona, J.; del Campo, J.; Lopez, G.; Mata, M.; Marsal, J. Water Consumption in Lysimeter-Grown Apple and Pear Trees with Different Training Systems. *Acta Hortic.* **2011**, *903*, 1181–1186. [CrossRef]
35. Zanotelli, D.; Montagnani, L.; Andreotti, C.; Tagliavini, M. Evapotranspiration and Crop Coefficient Patterns of an Apple Orchard in a Sub-Humid Environment. *Agric. Water Manag.* **2019**, *226*, 105756. [CrossRef]
36. Moran, M.S.; Jackson, R.D. Assessing the Spatial Distribution of Evapotranspiration Using Remotely Sensed Inputs. *J. Environ. Qual.* **1991**, *20*, 725–737. [CrossRef]
37. Allen, R.G.; Pereira, L.S.; Howell, T.A.; Jensen, M.E. Evapotranspiration Information Reporting: I. Factors Governing Measurement Accuracy. *Agric. Water Manag.* **2011**, *23*, 899–920. [CrossRef]
38. De la Fuente-Sáiz, D.; Ortega-Farías, S.; Fonseca, D.; Ortega-Salazar, S.; Kilic, A.; Allen, R. Calibration of METRIC Model to Estimate Energy Balance over a Drip-Irrigated Apple Orchard. *Remote Sens.* **2017**, *9*, 670. [CrossRef]
39. Raeini-Sarjaz, M.; Rostami, A. Remotely Sensed Measurements of Apple Orchard Actual Evapotranspiration and Plant Coefficient Using MODIS Images and SEBAL Algorithm (Case Study: Ahar Plain, Iran). *J. Agric. Meteorol.* **2016**, *4*, 32–43.
40. Pokorny, J. Evapotranspiration. In *Encyclopedia of Ecology*, 2nd ed.; Elsevier: Amsterdam, The Netherlands, 2019; pp. 292–303.
41. Odhiambo, L.O.; Irmak, S. Evaluation of the Impact of Surface Residue Cover on Single and Dual Crop Coefficient for Estimating Soybean Actual Evapotranspiration. *Agric. Water Manag.* **2012**, *104*, 221–234. [CrossRef]
42. Xing, N.; Huang, W.; Xie, Q.; Shi, Y.; Ye, H.; Dong, Y.; Wu, M.; Sun, G.; Jiao, Q. A Transformed Triangular Vegetation Index for Estimating Winter Wheat Leaf Area Index. *Remote Sens.* **2020**, *12*, 16. [CrossRef]
43. Gupta, H.; Kaur, L.; Asra, M.; Avtar, R.; Reddy, C.S. MODIS NDVI Multi-Temporal Analysis Confirms Farmer Perceptions on Seasonality Variations Affecting Apple Orchards in Kinnaur, Himachal Pradesh. *Agriculture* **2021**, *11*, 724. [CrossRef]
44. Zhu, Y.; Yang, G.; Yang, H.; Wu, J.; Lei, L.; Zhao, F.; Fan, L.; Zhao, C. Identification of Apple Orchard Planting Year Based on Spatiotemporally Fused Satellite Images and Clustering Analysis of Foliage Phenophase. *Remote Sens.* **2020**, *12*, 1199. [CrossRef]
45. Xue, J.; Su, B. Significant Remote Sensing Vegetation Indices: A Review of Developments and Applications. *J. Sens.* **2017**, *2017*, 1353691. [CrossRef]
46. Imran, H.A.; Gianelle, D.; Rocchini, D.; Dalponte, M.; Martín, M.P.; Sakowska, K.; Wohlfahrt, G.; Vescovo, L. VIS-NIR, Red-Edge and NIR-Shoulder Based Normalized Vegetation Indices Response to Co-Varying Leaf and Canopy Structural Traits in Heterogeneous Grasslands. *Remote Sens.* **2020**, *12*, 2254. [CrossRef]
47. Zheng, H.; Cheng, T.; Li, D.; Zhou, X.; Yao, X.; Tian, Y.; Cao, W.; Zhu, Y. Evaluation of RGB, Color-Infrared and Multispectral Images Acquired from Unmanned Aerial Systems for the Estimation of Nitrogen Accumulation in Rice. *Remote Sens.* **2018**, *10*, 824. [CrossRef]
48. Rabatel, G.; Gorretta, N.; Labbé, S. Getting Simultaneous Red and Near-Infrared Band Data from a Single Digital Camera for Plant Monitoring Applications: Theoretical and Practical Study. *Biosyst. Eng.* **2014**, *117*, 2–14. [CrossRef]
49. Mirzaee, S.; Mirzakhani Nafchi, A. Monitoring Spatiotemporal Vegetation Response to Drought Using Remote Sensing Data. *Sensors* **2023**, *23*, 2134. [CrossRef] [PubMed]
50. Panek, E.; Gozdowski, D. Analysis of Relationship Between Cereal Yield and NDVI for Selected Regions of Central Europe based on MODIS Satellite Data. *Remote Sens. Appl. Soc. Environ.* **2020**, *17*, 100286. [CrossRef]
51. Ferreira, S.; Sánchez, J.M.; Gonçalves, J.M. A Remote-Sensing-Assisted Estimation of Water Use in Rice Paddy Fields: A Study on Lis Valley, Portugal. *Agronomy* **2023**, *13*, 1357. [CrossRef]

52. Park, J.; Baik, J.; Choi, M. Satellite-Based Crop Coefficient and Evapotranspiration Using Surface Soil Moisture and Vegetation Indices in Northeast Asia. *CATENA* **2017**, *156*, 305–314. [CrossRef]
53. Lei, H.; Yang, D. Combining the Crop Coefficient of Winter Wheat and Summer Maize with a Remotely Sensed Vegetation Index for Estimating Evapotranspiration in the North China Plain. *J. Hydrol. Eng.* **2014**, *19*, 243–251. [CrossRef]
54. Lima, J. Water Requirement and Crop Coefficients of Sorghum in Apodi Plateau. *Rev. Bras. Eng. Agríc. Ambient.* **2021**, *25*, 684–688. [CrossRef]
55. Campos, I.; Neale, C.M.U.; Calera, A.; Balbontín, C.; González-Piqueras, J. Assessing Satellite-Based Basal Crop Coefficients for Irrigated Grapes (*Vitis vinifera* L.). *Agric. Water Manag.* **2010**, *98*, 45–54. [CrossRef]
56. Moreno, R.; Arias, E.; Sánchez, J.L.; Cazorla, D.; Garrido, J.; Gonzalez-Piqueras, J. HidroMORE 2: An Optimized and Parallel Version of HidroMORE. In Proceedings of the 2017 8th International Conference on Information and Communication Systems (ICICS), Irbid, Jordan, 4–6 April 2017; pp. 1–6.
57. Sánchez, N.; Martínez-Fernández, J.; Calera, A.; Torres, E.; Pérez-Gutiérrez, C. Combining Remote Sensing and In Situ Soil Moisture Data for the Application and Validation of a Distributed Water Balance Model (HIDROMORE). *Agric. Water Manag.* **2010**, *98*, 69–78. [CrossRef]
58. Garrido-Rubio, J.; Sanz, D.; González-Piqueras, J. Application of a Remote Sensing-Based Soil Water Balance for the Accounting of Groundwater Abstractions in Large Irrigation Areas. *Irrig. Sci.* **2019**, *37*, 709–724. [CrossRef]
59. Garrido-Rubio, J.; Calera, A.; Arellano, I.; Belmonte, M.; Fraile, L.; Ortega, T.; Bravo, R.; González-Piqueras, J. Evaluation of Remote Sensing-Based Irrigation Water Accounting at River Basin District Management Scale. *Remote Sens.* **2020**, *12*, 3187. [CrossRef]
60. Garrido-Rubio, J.; González-Piqueras, J.; Campos, I.; Osann, A.; González-Gómez, L.; Calera, A. Remote Sensing–Based Soil Water Balance for Irrigation Water Accounting at plot and Water User Association Management Scale. *Agric. Water Manag.* **2020**, *238*, 106236. [CrossRef]
61. Garrido-Rubio, J.; González-Piqueras, J.; Calera, A.; Osann, A. Remote Sensing-Based Green and Blue Agricultural Water Footprint Estimation at the River Basin Scale. *Ecol. Indic.* **2024**, *167*, 112643. [CrossRef]
62. Kottek, M.; Grieser, J.; Beck, C.; Rudolf, B.; Rubel, F. World Map of the Köppen-Geiger Climate Classification Updated. *Meteorol. Z.* **2006**, *15*, 259–263. [CrossRef]
63. Campar, A.; Gama, A.; Cunha, L.; Jacinto, R.; Boura, I.; Medeiros, J.; Brandão, J. *The Lis River Watershed—Contribution to the Study of Territory Organization and Environmental Problems*; Câmara Municipal de Leiria, CCDR-Centro: Coimbra, Portugal, 1989. (In Portuguese)
64. Ferreira, S.; Oliveira, F.; Gomes da Silva, F.; Teixeira, M.; Gonçalves, M.; Eugénio, R.; Damásio, H.; Gonçalves, J.M. Assessment of Factors Constraining Organic Farming Expansion in Lis Valley, Portugal. *AgriEngineering* **2020**, *2*, 111–127. [CrossRef]
65. CLIMATE-DATA.ORG. Clima Leiria. Available online: https://pt.climate-data.org/europa/portugal/leiria/leiria-140/ (accessed on 27 November 2024).
66. Gonçalves, J.M.; Ferreira, S.; Nunes, M.; Eugénio, R.; Amador, P.; Filipe, O.; Duarte, I.M.; Teixeira, M.; Vasconcelos, T.; Oliveira, F.; et al. Developing Irrigation Management at District Scale Based on Water Monitoring: Study on Lis Valley, Portugal. *AgriEngineering* **2020**, *2*, 78–95. [CrossRef]
67. Gonçalves, J.M.; Nunes, M.; Ferreira, S.; Jordão, A.; Paixão, J.; Eugénio, R.; Russo, A.; Damásio, H.; Duarte, I.M.; Bahcevandziev, K. Alternate Wetting and Drying in the Center of Portugal: Effects on Water and Rice Productivity and Contribution to Development. *Sensors* **2022**, *22*, 3632. [CrossRef] [PubMed]
68. Doorenbos, J.; Pruitt, W.O. *Crop Water Requirements*; Irrigation and Drainage Paper No. 24; FAO: Rome, Italy, 1997.
69. Allen, R.G.; Tasumi, M.; Morse, A.; Trezza, R.; Wright, J.L. Satellite-Based Energy Balance for Mapping Evapotranspiration with Internalized Calibration (METRIC)—Applications. *J. Irrig. Drain. Eng.* **2007**, *133*, 395–406. [CrossRef]
70. Laounia, N.; Abderrahmane, H.; Abdelkader, K.; Zahira, S.; Mansour, Z. Evapotranspiration and Surface Energy Fluxes Estimation Using the Landsat-7 Enhanced Thematic Mapper Plus Image over a Semiarid Agrosystem in the North-West of Algeria. *Rev. Bras. Meteorol.* **2017**, *32*, 691–702. [CrossRef]
71. IPMA. *Resumo Climatológico, Ano 2019*; IPMA: Lisbon, Portugal, 2019. Available online: https://www.ipma.pt/pt/publicacoes/boletins.jsp?cmbDep=cli&cmbTema=pcl&cmbAno=2019&idDep=cli&idTema=pcl&curAno=20 (accessed on 15 May 2024). (In Portuguese)
72. IPMA. *Resumo Climatológico, Ano 2020*; IPMA: Lisbon, Portugal, 2020. Available online: https://www.ipma.pt/pt/publicacoes/boletins.jsp?cmbDep=cli&cmbTema=pcl&cmbAno=2020&idDep=cli&idTema=pcl&curAno=20 (accessed on 15 May 2024). (In Portuguese)
73. IPMA. *Resumo Climatológico, Ano 2021*; IPMA: Lisbon, Portugal, 2021. Available online: https://www.ipma.pt/pt/publicacoes/boletins.jsp?cmbDep=cli&cmbTema=pcl&cmbAno=2021&idDep=cli&idTema=pcl&curAno=20 (accessed on 15 May 2024). (In Portuguese)
74. Maas, E.V.; Hoffman, G.J. Crop Salt Tolerance–Current Assessment. *J. Irrig. Drain. Div.* **1977**, *103*, 115–134. [CrossRef]

75. Ucar, Y.; Kocięcka, J.; Liberacki, D.; Rolbiecki, R. Analysis of crop water requirements for apple using dependable rainfall. *Atmosphere* **2023**, *14*, 99. [CrossRef]
76. Dragoni, D.; Lakso, A.N.; Piccioni, R.M. Transpiration of apple trees in a humid climate using heat pulse sap flow gauges calibrated with whole-canopy gas exchange chambers. *Agric. For. Meteorol.* **2005**, *130*, 85–94. [CrossRef]
77. Ebel, R.C.; Proebsting, E.L.; Evans, R.G. Deficit irrigation to control vegetative growth in apple and its effect on yield and fruit quality. *J. Am. Soc. Hortic. Sci.* **1995**, *120*, 571–578.
78. Naor, A. Irrigation and crop load influence fruit size and water relations in field-grown 'Golden Delicious' apple. *J. Am. Soc. Hortic. Sci.* **2001**, *126*, 546–550.
79. Cao, H.; Wang, H.; Li, Y.; Hamani, A.K.M.; Zhang, N.; Wang, X.; Gao, Y. Evapotranspiration Partition and Dual Crop Coefficients in Apple Orchard with Dwarf Stocks and Dense Planting in Arid Region, Aksu Oasis, Southern Xinjiang. *Agriculture* **2021**, *11*, 1167. [CrossRef]
80. Liu, C.; Sun, G.; McNulty, S.G.; Kang, S. An Improved Evapotranspiration Model for an Apple Orchard in Northwestern China. *Trans. ASABE* **2015**, *58*, 1253–1264. [CrossRef]
81. Rubauskis, E.; Berlands, V.; Jansons, V. Total evapotranspiration of apple trees with drip irrigation in high-density orchard. *Acta Hortic.* **2022**, *1335*, 153–162. [CrossRef]
82. Odi-Lara, M.; Campos, I.; Neale, C.M.U.; Ortega-Farías, S.; Poblete-Echeverría, C.; Balbontín, C.; Calera, A. Estimating Evapotranspiration of an Apple Orchard Using a Remote Sensing-Based Soil Water Balance. *Remote Sens.* **2016**, *8*, 253. [CrossRef]
83. Monaco, F.; Guido, S. How water amounts and management options drive Irrigation Water Productivity of rice. A multivariate analysis based on field experiment data. *Agric. Water Manag.* **2018**, *195*, 47–57. [CrossRef]
84. Gong, D.; Kang, S.; Yao, L.; Zhang, L. Estimation of evapotranspiration and its components from an apple orchard in northwest China using sap flow and water balance methods. *Hydrol. Process.* **2006**, *20*, 3173–3184. [CrossRef]
85. Calera, A.; Campos, I.; Osann, A.; D'Urso, G.; Menenti, M. Remote sensing for crop water management: From ET modelling to services for the end users. *Sensors* **2017**, *17*, 1104. [CrossRef]
86. Blatchford, M.L.; Karimi, P.; Bastiaanssen, W.G.M.; Nouri, H. From Global Goals to Local Gains—A Framework for Crop Water Productivity. *ISPRS Int. J. Geo. Inf.* **2018**, *7*, 414. [CrossRef]
87. Pouladi, P.; Badiezadeh, S.; Pouladi, M.; Yousefi, P.; Farahmand, H.; Kalantari, Z.; Yu, D.J.; Sivapalan, M. Interconnected governance and social barriers impeding the restoration process of Lake Urmia. *J. Hydrol.* **2021**, *598*, 126489. [CrossRef]
88. Diário da República. Presidency of the Council of Ministers No.77/2018. Republic Diary, 1st Series—No. 197—12 October 2018. Available online: https://files.dre.pt/1s/2018/10/19700/0494804957.pdf (accessed on 15 January 2024).
89. Licznar-Malanczuk, M.; Baluszynska, U.B. Do Living Mulches or Environmental Conditions Have a Greater Impact on the External Quality of the Apple Fruit 'Chopin' Cultivar? *Agriculture* **2024**, *14*, 610. [CrossRef]
90. Bhaskar, V.; Bellinder, R.R.; Reiners, S.; DiTommaso, A. Reduced Herbicide Rates for Control of Living Mulch and Weeds in Fresh Market Tomato. *Weed Technol.* **2020**, *34*, 55–63. [CrossRef]
91. Thorsted, M.D.; Olesen, J.E.; Weiner, J. Mechanical Control of Clover Improves Nitrogen Supply and Growth of Wheat in Winter Wheat/White Clover Intercropping. *Eur. J. Agron.* **2006**, *24*, 149–155. [CrossRef]
92. Association of Apple Producers of Alcobaça. ECOPOMAR Project: Sustainability in Apple Orchards. Available online: https://akisportugal.pt/grupos/ecopomar/documents/ (accessed on 29 November 2024).

Disclaimer/Publisher's Note: The statements, opinions and data contained in all publications are solely those of the individual author(s) and contributor(s) and not of MDPI and/or the editor(s). MDPI and/or the editor(s) disclaim responsibility for any injury to people or property resulting from any ideas, methods, instructions or products referred to in the content.